

# The Limited Impact of Medical Adaptation of Large Language and Vision-Language Models

Daniel P. Jeong<sup>1</sup>

DANIELJE@CS.CMU.EDU

Pranav Mani<sup>2</sup>

PRANAV@ABRIDGE.COM

Saurabh Garg<sup>3</sup>

GARG.SAURABH.2014@GMAIL.COM

Zachary C. Lipton<sup>1,2</sup>

ZLIPTON@CMU.EDU

Michael Oberst<sup>2,4</sup>

MOBERST@JHU.EDU

<sup>1</sup>Machine Learning Department, Carnegie Mellon University

<sup>2</sup>Abridge

<sup>3</sup>Mistral AI

<sup>4</sup>Department of Computer Science, Johns Hopkins University

## Abstract

Several recent works seek to adapt general-purpose large language models (LLMs) and vision-language models (VLMs) for medical applications through continued pretraining on publicly available biomedical corpora. These works typically claim that such domain-adaptive pretraining improves performance on various downstream medical tasks, such as answering medical exam questions. In this paper, we compare ten “medical” LLMs and two VLMs against their corresponding base models, arriving at a different conclusion: all medical VLMs and nearly all medical LLMs fail to consistently improve over their base models in the zero-/few-shot prompting and supervised fine-tuning regimes for medical question answering (QA). For instance, on clinical-note-based QA tasks in the 3-shot setting, medical LLMs outperform their base models in only 26.7% of cases, reach a (statistical) tie in 16.7% of cases, and perform significantly worse in the remaining 56.7% of cases. Our conclusions are based on (i) comparing each medical model directly against its base model; (ii) optimizing the prompts for each model separately in zero-/few-shot prompting; and (iii) accounting for statistical uncertainty in comparisons. Our findings suggest that state-of-the-art general-domain models may already exhibit strong medical knowledge and reasoning capabilities, and offer recommendations to strengthen the conclusions of future studies.

**Keywords:** domain-adaptive pretraining, large language models (LLMs), vision-language models (VLMs), foundation models for medical domain, question answering

## 1 Introduction

Recent advances in autoregressive large language models (LLMs) and vision-language models (VLMs) have attracted interest from practitioners in medicine, where these models hold great potential to transform various aspects of clinical practice (e.g., medical diagnosis, information retrieval from clinical documents, patient triaging) (Fries et al., 2022a; Moor et al., 2023a). State-of-the-art performance on various medical benchmarks is typically

achieved by massive-scale closed-source models, such as GPT-4 (OpenAI, 2023a,b), MEDGEMINI (Saab et al., 2024; Yang et al., 2024), and MED-PALM (Singhal et al., 2023a,b; Tu et al., 2024), often performing on par with humans on medical licensing exams and open-ended consumer health question-answering (QA) tasks. However, the general lack of transparency in these models, high API usage costs, and patient data privacy concerns make their integration into routine clinical workflows challenging (Marks and Haupt, 2023).

To address such concerns, recent works have proposed cheaper, open-source alternatives through *domain-adaptive pretraining* (DAPT; Gururangan et al., 2020), where a pretrained open-source general-domain model—such as LLAMA (Touvron et al., 2023a,b; Meta, 2024) or MISTRAL (Jiang et al., 2023) in the language space; and LLAVA (Liu et al., 2023) or OPEN-FLAMINGO (Awadalla et al., 2023) in the vision-language space—is continually pretrained on biomedical (image-)text corpora from public sources such as PubMed. While some works show that medical models pretrained from scratch only using domain-specific corpora can outperform those trained via DAPT, both in the context of BERT-style encoder-only models (Devlin et al., 2019; Gu et al., 2021; Yang et al., 2022) and decoder models (Taylor et al., 2022; Luo et al., 2022; Hernandez et al., 2023; Bolton et al., 2024), the DAPT approach has become common practice, resulting in a trend where the release of a more capable general-domain model is typically followed by the release of its medical counterpart.

Despite the widespread adoption of medical DAPT, the claimed improvements in performance are worth scrutinizing. While the central story (improved domain-specific performance through domain-specific adaptation) is intuitive, more recent base models often already exhibit strong off-the-shelf performance on medical benchmarks without any adaptation. For instance, as of the time of writing, the general-domain LLAMA-3-8B (Meta, 2024) outperforms other medically specialized models such as MEDI TRON-70B (Chen et al., 2023) and BIOMISTRAL-7B (Labrak et al., 2024) on the Open Medical LLM Leaderboard (Pal et al., 2024), which evaluates each model on standard medical QA benchmark datasets such as MedQA (Jin et al., 2020) and MedMCQA (Pal et al., 2022). Moreover, given the general lack of transparency about the pretraining corpora used to train the general-domain model in the first place, it is possible that they may already be trained on relevant medical text (or even the very same text as used for medical DAPT).

Perhaps more concerning is the lack of apples-to-apples comparisons in the literature. First, medical models resulting from DAPT are often only compared against other baselines with different architectures and model scale (e.g., CLINICAL-CAMEL-70B (Toma et al., 2023) vs. GPT-4 (OpenAI, 2023a)). Second, even for the same model scale, models are often evaluated under inconsistent evaluation setups. For example, Chen et al. (2023) fine-tune MEDI TRON-70B on MedMCQA with gradient updates and compare it to CLINICAL-CAMEL-70B (Toma et al., 2023) zero-shot prompted on MedMCQA. Third, the common practice of using a single, fixed prompting setup (e.g., prompt format, choice of few-shot examples) for all models under evaluation also warrants concern, as LLM/VLM behavior is extremely sensitive to such design decisions (Jiang et al., 2020; Zhao et al., 2021; Ceballos-Arroyo et al., 2024), and prompt designs optimized for a proposed method are seldom optimal for the baselines (Sclar et al., 2024). These issues can undermine the validity of claimed performance benefits in the medical DAPT literature.

Meanwhile, medical LLMs trained via DAPT are often solely evaluated on QA tasks designed to assess medical knowledge (e.g., MedQA (Jin et al., 2020), MedMCQA (Pal et al.,

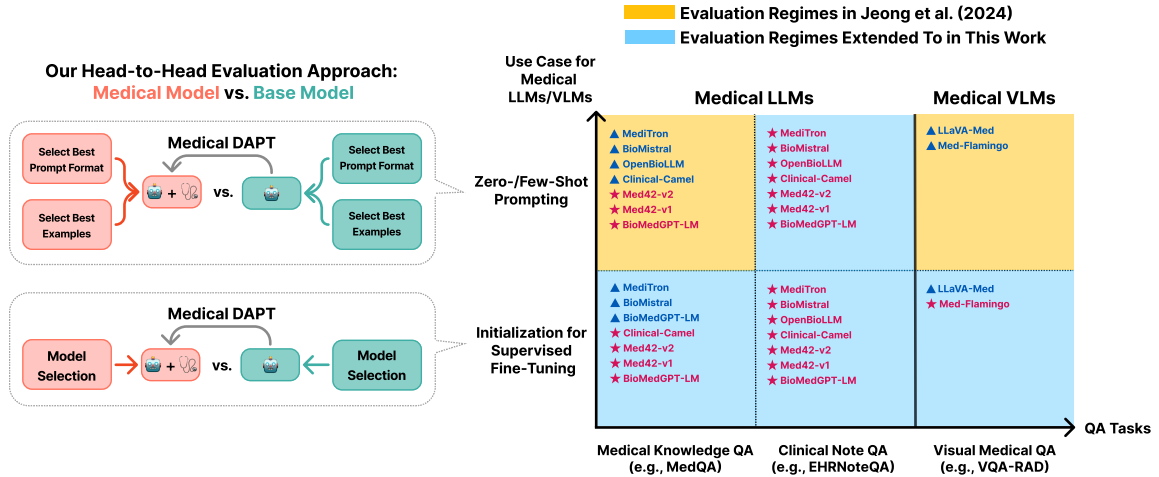


Figure 1: Overview of our head-to-head evaluation approach for each pair of medical LLM/VLM (red) and its base model (turquoise), across a wide variety of medical QA tasks and model use cases. (Left) We compare each model pair based on their zero-/few-shot QA capabilities (top) and their QA performances after supervised fine-tuning (bottom), *while ensuring that their only differences lie in medical DAPT*. (Right) We substantially extend the results of Jeong et al. (2024) (yellow) to include QA tasks based on clinical notes, as well as a comparison of downstream QA performance when using medical vs. general-domain models as an initialization for fine-tuning (cyan). Within each evaluation regime, a  $\blacktriangle$  indicates that a model is evaluated in that regime both in the original paper and in our work, while a  $\star$  indicates that it is *only* evaluated in our work<sup>1</sup>. *None of the medical LLMs we evaluate have previously been evaluated on QA tasks based on real-world clinical notes.*

2022)), although it is generally unclear whether strong performance on such tasks necessarily implies high clinical utility (Wornow et al., 2023). Notably, clinical notes (e.g., outpatient SOAP notes and discharge summaries) look different from academic biomedical articles (PubMed is the primary source of data used in many medical adaptation papers (Table 2)) both in form, content, and surface-level use of language (e.g., syntactical differences, use of jargon, abundance of naturally occurring grammatical errors (Agrawal et al., 2022; Hernandez et al., 2023)). To assess whether medical DAPT contributes to higher clinical utility, it is essential to also evaluate medical models resulting from DAPT on QA tasks grounded on real-world clinical notes in direct comparison against their base models.

In this paper, we perform an apples-to-apples comparison that addresses these concerns, comparing ten medical LLMs and two medical VLMs against their general-domain base models on various medical (visual) QA tasks (Figure 1). For each pair of general-domain and medically adapted LLMs/VLMs, **whose only differences lie in medical DAPT** (i.e., one model is the base model, from which the other is derived via medical DAPT), we compare their downstream performances from (i) zero-/few-shot prompting (Radford et al.,

1. Although Christophe et al. (2024a,b) describe their evaluation of the proposed MED42 models on medical knowledge QA tasks as being in the “zero-shot” setting, we treat the zero-/few-shot prompting evaluations as missing, since they were already fine-tuned on these datasets via medical DAPT.

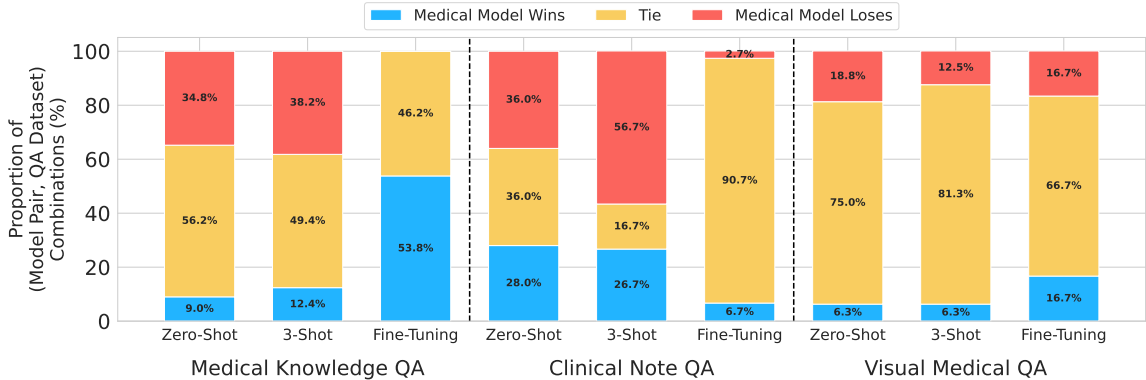


Figure 2: Medical LLMs and VLMs trained via DAPT show limited improvement over their general-domain counterparts in the zero-/few-shot prompting and supervised fine-tuning (SFT) regimes. Here, we show the win, tie, and loss rates (%) of medical models vs. their corresponding base models across all (model pair, QA dataset) combinations. Win rate refers to the proportion of (model pair, QA dataset) combinations where a medical model shows a *statistically significant* improvement. We do observe that on textual medical knowledge QA tasks, medical LLMs outperform their base models in the SFT regime, although the improvements are marginal (1.6% average gain in accuracy; Section 5.1).

2019; Brown et al., 2020) and (ii) supervised fine-tuning (SFT). For the former, we follow Jeong et al. (2024) and compare the performances after independently selecting the “best” prompt format and few-shot examples for each model based on the validation set (Section 3.1). For the latter, we compare the performances after fine-tuning each model on the training set of each downstream QA dataset, using the best hyperparameters selected via grid search (Section 3.2). In both cases, we use the percentile bootstrap to assess whether the perceived improvements in performance from medical DAPT are attributable to chance. In Table 2, we list all of the LLM/VLM pairs included in our study, which were selected to cover a wide range of general-domain base models and model scales (7B–70B).

**Overall, we find that both medical LLMs and VLMs show limited improvement over their base models, across all of the medical QA tasks and evaluation settings that we consider (Figure 2).** In the zero-/few-shot prompting regime (Section 4), we find that all medical VLMs and the majority of medical LLMs fail to consistently outperform their base models across all datasets, including QA tasks focused on assessing medical knowledge and those based on real-world clinical notes. In the SFT regime (Section 5), we find that the medical LLMs overall *do* show statistically significant improvements on the medical knowledge QA tasks but not on the clinical note QA tasks, while the medical VLMs show little to no improvement on all of the visual medical QA tasks. Our findings suggest that a rigorous pairwise comparison of models, including tests for statistical significance, is essential to draw reliable conclusions about the performance benefits from medical DAPT, while these basic practices are not consistently adopted in the literature (Table 1).

Our main contributions can be summarized as follows:

Table 1: Prior works overlook aspects critical to assessing the impact of medical DAPT on downstream zero-/few-shot performance, potentially leading to overly optimistic conclusions about its benefits. For each medical LLM/VLM included in our study (Table 2), we summarize the following details: (i) whether the medical model was compared against its base model; (ii) whether the sensitivity of the medical model and its base model to the choice of prompt format and few-shot examples was considered in their comparison; and (iii) whether statistical tests were performed to determine the significance of any measured performance improvement.  $\blacktriangle$  indicates that the corresponding aspect was only partially considered (e.g., accounted for sensitivity to few-shot examples but not the prompt format).

	Compared to Base Model?	Accounted for Prompt Sensitivity?	Tested for Statistical Significance?
MED42-v2 (Christophe et al., 2024b)	✓		
MED42-v1 (Christophe et al., 2024a)	✓		
OPENBIO-LLM (Pal and Sankarasubbu, 2024)			
CLINICAL-CAMEL (Toma et al., 2023)			
BIO-MISTRAL (Labrak et al., 2024)	✓		$\blacktriangle$
MEDI-TRON (Chen et al., 2023)	✓		$\blacktriangle$
BIO-MEDGPT-LM (Luo et al., 2023)			
LLAVA-MED (Li et al., 2023a)	✓		
MED-FLAMINGO (Moor et al., 2023b)	✓		
<b>Our Evaluation</b>	✓	✓	✓

1. We provide a comprehensive head-to-head comparison between state-of-the-art general-domain LLMs/VLMs and their medical DAPT counterparts on a wide range of medical QA tasks, to investigate the effectiveness of DAPT for medical specialization.
2. We find that when the prompts are optimized for each medical and general-domain model independently, the majority of medical models fail to improve over their general-domain counterparts in the zero-/few-shot prompting regime (Section 4.1).
3. We show that using a single, fixed prompt format and choice of few-shot examples for all models without statistical testing can lead to overly optimistic conclusions about the benefits from medical DAPT in the zero-/few-shot prompting regime (Section 4.2).
4. We find that in the SFT regime, all medical VLMs fail to show improvement, while medical LLMs show improvement on textual medical knowledge QA tasks but not on QA tasks based on real-world clinical notes (Section 5).

## 2 Related Work

DAPT (Gururangan et al., 2020) is a transfer learning approach, where a pretrained model is further pretrained on domain-specific data for better alignment to a target domain of interest (e.g., medicine, law). Several studies show that language models trained via DAPT often outperform their general-domain counterparts on domain-specific tasks, such as claim detection from blog posts (Chakrabarty et al., 2019), named entity recognition from German novels (Konle and Jannidis, 2020), and judgment prediction for legal cases (Xiao et al., 2021). In the medical domain, prior works based on BERT-style encoder models (Devlin et al., 2019), such as BIOBERT (Lee et al., 2019) and CLINICALBERT (Alsentzer et al., 2019), show that medical DAPT improves fine-tuning performance on tasks such as medical

concept extraction from patient reports (Uzuner et al., 2011), identification of gene-disease relations from PubMed abstracts (Doğan et al., 2014; Bravo et al., 2015; Krallinger et al., 2017), and natural language inference on clinical notes (Romanov and Shivade, 2018).

More recent works suggest that decoder-based autoregressive LLMs and VLMs trained via medical DAPT also show strong performance on various downstream medical tasks. Medical LLMs such as MEDITRON (Chen et al., 2023), adapted from LLAMA-2 (Touvron et al., 2023b); and BIOMISTRAL (Labrak et al., 2024), adapted from MISTRAL-7B-INSTRUCT-V0.1 (Jiang et al., 2023); perform well on knowledge-intensive QA tasks derived from medical licensing and academic exams (Jin et al., 2020; Pal et al., 2022; Hendrycks et al., 2021) and PubMed abstracts (Jin et al., 2019). Medical VLMs such as LLAVA-MED (Li et al., 2023a), adapted from LLAVA (Liu et al., 2023); and MED-FLAMINGO (Moor et al., 2023b), adapted from OPEN-FLAMINGO (Awadalla et al., 2023); also perform well on visual medical QA tasks based on radiology (Lau et al., 2018; Liu et al., 2021) and pathology images (He et al., 2020) and academic exams (Yue et al., 2024). These encouraging results have established DAPT as a go-to approach for training medically specialized LLMs and VLMs, a conclusion that we re-examine across different evaluation settings (zero-/few-shot prompting, SFT) and across both knowledge-intensive and clinically relevant QA tasks.

### 3 Experimental Setup

To investigate the effectiveness of medical DAPT in improving (i) zero-/few-shot and (ii) SFT performances, we compare ten medical LLMs and two medical VLMs against their general-domain counterparts in *pairs* on 22 textual medical QA datasets (8 based on clinical notes) and 8 visual medical QA datasets, respectively (Figure 1). The models in each pair are *exactly identical* in model architecture and scale, and their only difference lies in whether they were additionally pretrained on medical data. We also note that while some of the datasets considered contain both closed-ended questions (with objective ground-truth answers) and open-ended questions, we focus our evaluations on the former, where an objective, quantitative assessment of medical knowledge and reasoning capabilities is possible. To ensure the reproducibility of our results, we open-source the source code used for all of our evaluations described below via our GitHub repository<sup>2</sup>.

**Models (Table 2).** For medical LLM evaluations, we consider the following model families: MED42-v2 (Christophe et al., 2024b), MED42-v1 (Christophe et al., 2024a), OPENBIO-OLLM (Pal and Sankarasubbu, 2024), MEDITRON (Chen et al., 2023), CLINICAL-CAMEL (Toma et al., 2023), BIOMISTRAL (Labrak et al., 2024), and BIOMEDGPT-LM (Luo et al., 2023). For medical VLM evaluations, we consider LLAVA-MED (Li et al., 2023a) and MED-FLAMINGO (Moor et al., 2023b). For all models, we use the checkpoints made available via HuggingFace. In all zero-/few-shot prompting experiments, we generate predictions from each model via (i) greedy decoding (i.e., sampling with temperature  $T = 0$ ) and (ii) constrained decoding. For constrained decoding, we constrain the token vocabulary to be one of the answer choice letters (e.g., one of [“A”, “B”, “C”, “D”] for a four-choice QA dataset) and treat the answer choice with the highest token probability as a given model’s prediction. For

---

2. [github.com/taekb/eval-medical-dapt](https://github.com/taekb/eval-medical-dapt)

Table 2: Summary of open-source autoregressive VLM and LLM pairs used for evaluation. For MED42, we only list the top-five adaptation datasets with the highest mixture ratios.

Model Class	General Domain	Medical Domain	Medical Adaptation Corpora
LLM	LLAMA-3-70B-INSTRUCT	MED42-v2-70B	Medical QA Datasets (e.g., MedQA, MedMCQA) Medical Instruction 120k (Altaf, 2023) OpenGPT (OpenChat) (Wang et al., 2024) StackExchange (Lambert et al., 2023) Medical Flashcards (Han et al., 2023)
			Undisclosed
			Clinical Practice Guidelines (e.g., CDC, WHO) PubMed Articles (S2ORC; Lo et al., 2020)
			ShareGPT 20k PubMed Articles Published Before 2021 Random 4k Subset of MedQA (Jin et al., 2020)
			Medical QA Datasets (e.g., MedQA, MedMCQA) OpenGPT (OpenChat) (Wang et al., 2024) StackExchange (Lambert et al., 2023) Medical Flashcards (Han et al., 2023) CORD-19 (Wang et al., 2020)
	LLAMA-2-70B	CLINICAL-CAMEL-70B	Medical QA Datasets (e.g., MedQA, MedMCQA) OpenGPT (OpenChat) (Wang et al., 2024) StackExchange (Lambert et al., 2023) Medical Flashcards (Han et al., 2023) CORD-19 (Wang et al., 2020)
			Undisclosed
			Clinical Practice Guidelines (e.g., CDC, WHO) PubMed Articles (S2ORC; Lo et al., 2020)
			PubMed Articles (PMC Open Access Subset)
			PubMed Articles (S2ORC; Lo et al., 2020)
VLM	LLAVA-v0-7B	LLAVA-MED-7B	PubMed Articles (PMC-15M; Zhang et al., 2023)
	OPEN-FLAMINGO-9B	MED-FLAMINGO-9B	Medical Textbooks (MTB; Moor et al., 2023b) PubMed Articles (PMC-OA; Lin et al., 2023)

the SFT experiments, we only generate predictions via greedy decoding, as it best reflects the setup used for fine-tuning (Section 3.2).

**Textual Medical Knowledge QA Datasets.** For textual medical knowledge QA, we use MedQA (Jin et al., 2020), MedMCQA (Pal et al., 2022), PubMedQA (Jin et al., 2019), and MMLU-Medical (Hendrycks et al., 2021) for evaluation. MMLU-Medical refers to a subset of MMLU corresponding to 9 subjects related to medicine: anatomy, clinical knowledge, college biology, college medicine, high school biology, medical genetics, nutrition, professional medicine, and virology. For MedQA, we use the official train-validation-test splits as provided through BigBio (Fries et al., 2022b). We note that MedQA has two versions, one with four answer choices per question and the other with five, and we use both for evaluation. For MedMCQA, which does not have a public test set, we follow the approach taken by Wu et al. (2024) and Labrak et al. (2024), taking a random 80–20 train-validation split of the official training set and using the official validation set for testing. For PubMedQA, we follow Singhal et al. (2023a), using the 211k artificially generated QA samples for training,

and taking a 50–50 split on the 1k expert-labeled examples. For MMLU-Medical, we use the official split as provided. Meanwhile, as the MED42 models—MED42-v2-70B, MED42-v2-8B, and MED42-v1-70B—were trained on all of the QA datasets mentioned above as part of DAPT, *we exclude these models from our discussion on textual medical knowledge QA*.

**Textual Clinical Note QA Datasets.** As strong performance on medical knowledge QA tasks may not necessarily imply high clinical utility (Wornow et al., 2023), we also perform evaluations with the following textual QA datasets based on clinical notes: MedNLI (Romanov and Shivade, 2018), EHRNoteQA (Kweon et al., 2024), the 2008 i2b2 Obesity Comorbidity Detection Challenge dataset (Uzuner, 2009) (4 classification tasks), the CASI Clinical Acronym Sense Disambiguation dataset (Moon et al., 2014), and the MIMIC-III Clinical Acronym Sense Disambiguation dataset (Johnson et al., 2016; Adams et al., 2020). For MedNLI, we frame each natural language inference task as a three-way closed-ended QA task, where the answer to each question is one of [“entailment”, “contradiction”, and “neutral”], and use the official train–validation–test splits provided via PhysioNet (Goldberger et al., 2000) under a data use agreement. For EHRNoteQA, we use the “Level 1” subset, which only contains QA pairs with clinical notes at most 3k tokens in length, to account for the limited context window sizes of the LLMs that we evaluate, and take a random 60–20–20 split of the data to obtain the train, validation, and test sets. For the 2008 i2b2 Obesity Comorbidity Detection Challenge dataset, we follow the preprocessing steps in Ceballos-Arroyo et al. (2024) to obtain 4 binary classification (i.e., two-way multiple-choice QA) datasets, each focused on detecting the presence of (i) asthma, (ii) coronary artery disease (CAD), (iii) diabetes, and (iv) obesity from a given clinical note. We then select the QA pairs with clinical notes at most 3k tokens in length, as done for EHRNoteQA. As the preprocessing pipeline by Ceballos-Arroyo et al. (2024) outputs a train–test split, we take a random 80–20 split on the training set to obtain the train and validation sets. For the CASI and MIMIC-III sense disambiguation datasets, we follow the preprocessing steps detailed in Adams et al. (2020) for consistency with prior works (Agrawal et al., 2022).

**Visual Medical QA Datasets.** For visual medical QA, we use VQA-RAD (Lau et al., 2018), PathVQA (He et al., 2020), SLAKE (Liu et al., 2021), and MMMU-Medical (Yue et al., 2024) for evaluation. MMMU-Medical is a subset of MMMU with 5 subjects relevant to medicine: basic medical science, clinical medicine, diagnostics and lab medicine, pharmacy, and public health. For VQA-RAD, we address the train–test leakage and duplication issues in the official train–test split (Moor et al., 2023b) by removing the training examples repeated in the test set and removing all duplicates in both sets. As the official split does not include a validation set, we take a random 80–20 split on the training set to create a new train–validation split. For MMMU-Medical, which lacks a public test set, we randomly select 5 examples from the official validation set for validation, and reserve the remaining 25 examples for testing. For all other datasets, we use the official split as provided.

**Evaluation Metric.** Since we focus on closed-ended QA tasks, we use exact-match accuracy as our main evaluation metric. Following the Holistic Evaluation of Language Models (HELM) benchmark (Liang et al., 2023), we treat the text generated by a model (without any constraints on the vocabulary) to be its prediction, and check for an exact match between the prediction and the correct answer up to primitive string operations (e.g., lower-casing, removing white space/punctuation). If multiple matches occur, we treat the prediction

as incorrect (even if one of the matches is the correct answer), in order to handle cases where the model simply repeats the list of answer choices or produces an ambiguous answer (e.g., selecting multiple answer choices). Meanwhile, to quantify the extent of *improvement* from medical DAPT, we also consider the *relative* accuracy of the medical model with respect to the general-domain model. Formally, we define relative exact-match accuracy as  $\mathbb{E}[\mathbf{1}[f_{\text{medical}}(x) = y] - \mathbf{1}[f_{\text{general}}(x) = y]] \in [-1, 1]$ , where  $f_{\text{medical}}$  and  $f_{\text{general}}$  denote the medical and general-domain models,  $x$  and  $y$  denote the input prompt and answer in a QA pair from the test set, and  $\mathbf{1}[\cdot]$  denotes the indicator function. This metric quantifies the difference in accuracy between the medical model and the general-domain model. We refer to the accuracy of a particular model as the *absolute* exact-match accuracy in subsequent discussions, and refer to the metric above (for a pair of models) as the *relative* accuracy.

**Assessing Statistical Significance.** Given the relatively small size of test datasets in medical QA benchmarks, it is important to assess whether the perceived improvements in performance from medical DAPT are attributable to chance. To account for statistical uncertainty, we use the percentile bootstrap, re-sampling (with replacement) questions from the test set to get a sample of the same size as the original test set. Within each resample, we compute the difference in accuracy for the paired models, and repeat this process for 10,000 iterations. The resulting distribution of relative accuracy is used to derive a 95% confidence interval, and we judge a difference to be statistically significant if this interval does not cross zero. We do not perform any type of multiple-testing correction, which would have the effect of lowering the number of comparisons deemed to be significant.

### 3.1 Zero-/Few-shot Prompting with Model-Specific Prompt Selection

In this section, we provide an overview of our approach to assess whether medical DAPT leads to statistically significant improvements in zero-/few-shot medical QA performance. For few-shot prompting, we consider the 3-shot setting to ensure that the input prompt is shorter than the context window sizes for all models evaluated. Meanwhile, we exclude the EHRNoteQA and i2b2 datasets from few-shot prompting evaluations for medical LLMs, as most of the clinical notes in these datasets already occupy the full context window for most models even in the zero-shot setting. For evaluation, we pay special attention to two aspects. First, language models are highly sensitive to the choice of prompting strategy (e.g., prompt format, choice of few-shot examples), where seemingly insignificant changes to the prompt can lead to idiosyncratic model behavior (Jiang et al., 2020; Zhao et al., 2021; Ceballos-Arroyo et al., 2024). Second, prior works show that the “optimal” choice of prompt format is rarely the same between different models (Sclar et al., 2024), suggesting that using a single, fixed prompt for all models for comparison can result in misleading conclusions.

To ensure a fair comparison that isolates the impact of medical DAPT, we treat the choice of prompt format and few-shot examples as additional hyperparameters when generating predictions, and tailor them to each model *independently* (Figure 3). We first randomly sample 10 plausible prompt formats from a predefined search space and 10 different sets of few-shot examples from the training set of each dataset. We then search over all pairs of prompt formats (plus one additional manually designed default format) and few-shot examples, and select the best pair out of  $(10 + 1) \times 10 = 110$  that results in the highest validation exact-match accuracy. Given that a grid search at this scale can be computationally ex-

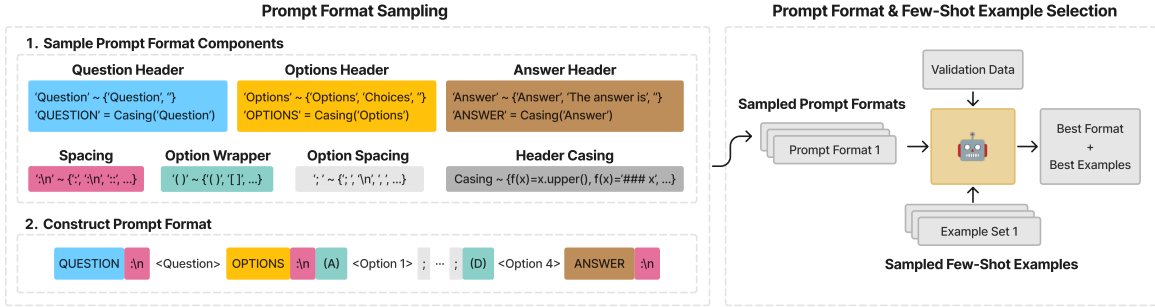


Figure 3: Overview of the prompt format sampling (left) and model-specific prompt selection (right) process considered in our evaluations (Section 3.1).

pensive, especially for datasets like MedMCQA that contain 37k validation QA pairs (Table A1), we randomly subsample 500 validation QA pairs for datasets that have more than 500. Using the vLLM framework (Kwon et al., 2023) for sampling model outputs, this leads to a runtime of around 5–15 minutes per trial, when using 4 NVIDIA A6000 GPUs for the 70B models and 2 GPUs for the others. We then generate the final predictions on the test set using the prompt format and few-shot samples selected for each model. In the zero-shot setting, we only search over the prompt formats. Meanwhile, we acknowledge that in the “truly” zero-shot setting, it may not be possible to optimize the prompt with respect to a dedicated validation set. Nonetheless, we implement our prompt selection approach even in the zero-shot setting to mitigate the potential impact that choosing a particular prompt format has on QA performance, and ensure a fair comparison between models in each pair.

To define the prompt format search space, we follow Sclar et al. (2024) and construct a context-free grammar of semantically equivalent yet syntactically distinct prompt formats (Figure 3, left). For the medical models that have a specific prompt format designed and recommended for closed-ended QA tasks (e.g., BIOMISTRAL (Labrak et al., 2024)), we fix the prompt format to what is provided and only search over the choice of few-shot examples. When such information is missing or only partially available (Table C1), we search over both the prompt formats and few-shot examples. For instruction-tuned models, which typically have a structured conversational format that is expected (e.g., “### User:...### Assistant:...”), we use the sampled question and answer templates to format each “user” query and “assistant” response. We provide the remaining details in Appendices B–C.

### 3.2 Supervised Fine-Tuning (SFT)

To assess whether medical DAPT leads to a better initialization of the model parameters for fine-tuning on downstream medical QA tasks, we compare the performances of models in each pair after fine-tuning each on the training set of each QA dataset. Due to computational constraints, we focus on parameter-efficient fine-tuning methods (detailed below) instead of full fine-tuning. For the textual medical QA evaluations, we exclude the MMLU-Medical datasets given that the training sets only include 5 examples per subject. For the visual medical QA evaluations, we exclude the MMMU-Medical datasets for the same reason.

**Parameter-efficient fine-tuning.** For MED-FLAMINGO-9B and OPEN-FLAMINGO-9B, we fine-tune the gated cross-attention layers, the Perceiver resampler (Jaegle et al., 2021), and the embeddings of the special `<image>` and `<|endofchunk|>` tokens, which correspond to a only subset of all model parameters. For all other LLMs and VLMs, we fine-tune each model with low-rank adapters (LoRA; Hu et al., 2022). We add the low-rank adapters to all of the linear layers (i.e., the self-attention and feedforward network layers in each Transformer block), following prior works that demonstrate its effectiveness over adapting a subset of the linear layers (Dettmers et al., 2023; Biderman et al., 2024). We fine-tune the trainable parameters by minimizing the cross-entropy loss on the output tokens generated conditional on the input context (i.e., the task instruction, image, and question). We train all models for a maximum of 10 epochs and apply early stopping regularization, monitoring the validation loss after every epoch of training and enforcing a patience of 1. To apply the gradient updates, we use the AdamW optimizer (Loshchilov and Hutter, 2019) with the recommended momentum hyperparameters  $\beta_1 = 0.9$ ,  $\beta_2 = 0.999$ , and  $\epsilon = 10^{-8}$  (Kingma and Ba, 2015); and a cosine learning rate schedule with a linear warmup of  $0.05 \times$  maximum number of training steps. For MED-FLAMINGO-9B and OPEN-FLAMINGO-9B, we perform a grid search over the learning rates and weight decay coefficients and use the validation loss to select the best setting for final evaluation. For all other models, we perform a grid search over the LoRA ranks and learning rates and use the validation loss to select the best setting. We perform all experiments using the DeepSpeed ZeRO (Rajbhandari et al., 2020) and PyTorch FSDP (Zhao et al., 2023) frameworks for distributed training. Meanwhile, for fine-tuning the 70B-parameter LLMs on PubMedQA and i2b2 (Diabetes), we also apply 4-bit NormalFloat double quantization (QLoRA; Dettmers et al., 2023) to the model parameters to address out-of-memory issues. We provide the remaining details in Appendix E.

## 4 Zero-/Few-Shot Prompting Evaluation Results

We summarize the main findings from the zero-/few-shot prompting experiments outlined in Section 3.1. Unless specified otherwise, we focus on the greedy decoding results in subsequent discussions and include the results for constrained decoding in Appendix D. **Overall, we find that all medical VLMs and the majority of medical LLMs fail to consistently improve over their general-domain counterparts in the zero-/few-shot prompting regime (Section 4.1).** We find that the medical LLMs do not show consistent improvements on *either* medical knowledge QA or clinical note QA datasets in this setting. Moreover, we demonstrate the importance of rigorous experimental design in surfacing this finding—performing pairwise model comparison with a single, fixed prompt optimized only for the medical model, while ignoring statistical uncertainty, can paint a misleadingly optimistic picture of off-the-shelf performance benefits from medical DAPT (Section 4.2).

### 4.1 Performance Benefits from Medical DAPT Largely Diminish After Model-Specific Prompt Selection and Statistical Testing

We first show that all medical VLMs and the majority of medical LLMs fail to consistently outperform their corresponding base models in terms of zero-shot and 3-shot performance, after model-specific prompt selection and statistical testing. We calculate the 95% confidence intervals in relative exact-match accuracy via bootstrapping on the test set, as described in

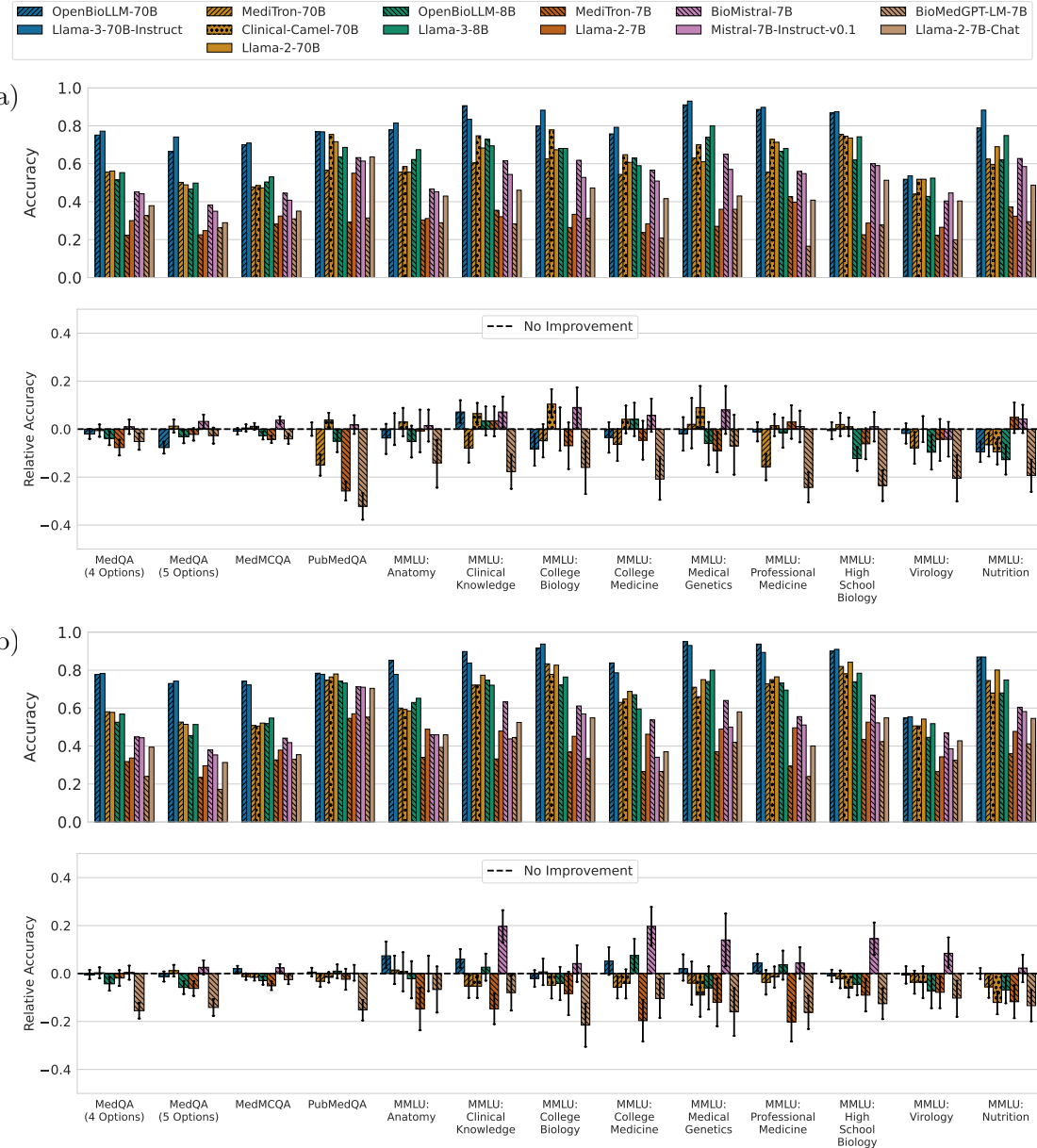


Figure 4: After independently selecting the best prompt format and examples for each model, medical LLMs (textured bars) fail to consistently improve over their base models (solid bars) on textual medical knowledge QA tasks, in both (a) zero-shot and (b) 3-shot settings. In each panel, the top row shows the absolute exact-match accuracies on the test set, and the bottom row shows the relative exact-match accuracies along with 95% confidence intervals derived via bootstrapping on the test set (Section 3). Here, model predictions are generated via greedy decoding. Improvements are also limited with constrained decoding (Figure D1).

Section 3. Below, we present the results on the textual medical knowledge QA datasets, the textual clinical note QA datasets, and the visual medical QA datasets one-by-one.

Table 3: The zero-shot and 3-shot win/tie/loss rates (%) for all medical LLMs on textual medical knowledge QA, after independently optimizing the prompt for each model. For each medical model, we boldface the win rate if it wins more than it loses to its general-domain base model, and vice versa. Here, we show the results when model predictions are generated via greedy decoding. The results for constrained decoding are shown in Table D1.

Model	Zero-Shot			3-Shot		
	Win	Tie	Loss	Win	Tie	Loss
OPENBIO-LLM-70B	7.7	69.2	<b>23.1</b>	<b>30.8</b>	69.2	0
MEDI-TRON-70B	0	61.5	<b>38.5</b>	0	69.2	<b>30.8</b>
CLINICAL-CAMEL-70B	<b>27.3</b>	63.6	9.1	0	63.6	<b>36.4</b>
OPENBIO-LLM-8B	0	46.2	<b>53.8</b>	7.7	61.5	<b>30.8</b>
MEDI-TRON-7B	0	69.2	<b>30.8</b>	0	23.1	<b>76.9</b>
BIO-MISTRAL-7B	<b>30.8</b>	69.2	0	<b>46.2</b>	53.8	0
BIO-MEDGPT-LM-7B	0	15.4	<b>84.6</b>	0	7.7	<b>92.3</b>
Aggregate	9.0	56.2	<b>34.8</b>	12.4	49.4	<b>38.2</b>

#### 4.1.1 EVALUATION OF MEDICAL LLMs ON TEXTUAL MEDICAL KNOWLEDGE QA

In Figures 4(a) and (b), we show the absolute and relative exact-match accuracies achieved by the medical and general-domain LLMs on the textual medical knowledge QA datasets, from zero-shot and 3-shot prompting, respectively. In Table 3, we show the win, tie, and loss rates (%) of the medical LLMs, where win rate refers to the proportion of QA datasets where a medical model shows a statistically significant improvement over its base model. We exclude the results for CLINICAL-CAMEL-70B on both versions of MedQA, and the MED42 models on all textual medical knowledge QA datasets, as they have already been trained on these datasets as part of medical DAPT (Table 2).

Overall, we find that the majority of medical models show little to no improvement over their base models, with the 95% confidence intervals in relative accuracy crossing or lying below zero (bottom rows of Figure 4(a) and (b)). In fact, **in each setting (zero-shot and 3-shot), only 2 out of 7 medical LLMs show statistically significant improvements** in performance (i.e., win more than they lose to their base models), and **only one medical LLM shows statistically significant improvements in both settings** (Table 3). In the zero-shot setting, only CLINICAL-CAMEL-70B (**orange**) and BIO-MISTRAL-7B (**purple**) show improvements, each achieving win/tie/loss rates of 27.3%/63.6%/9.1% and 30.8%/69.2%/0%, respectively. In the 3-shot setting, only OPENBIO-LLM-70B (**blue**) and BIO-MISTRAL-7B (**purple**) show significant improvements, each achieving win/tie/loss rates of 30.8%/69.2%/0% and 46.2%/53.8%/0%, respectively. Notably, BIO-MISTRAL-7B is the only medical LLM that consistently outperforms its base model (MISTRAL-7B-INSTRUCT-v0.1) across both settings, albeit with relatively low absolute performance.

Meanwhile, we observe that some medical LLMs actually perform significantly worse than their base models—e.g., MEDI-TRON-7B and BIO-MEDGPT-LM-7B with loss rates of 76.9% and 92.3% in the 3-shot setting. When we aggregate the results over all (model pair, textual medical knowledge QA dataset) combinations (last row of Table 3), we find that the medical LLMs achieve win/tie/loss rates of 9.0%/56.2%/34.8% in the zero-shot setting and

12.4%/49.4%/38.2% in the 3-shot setting, indicating that the medical LLMs overall reach a statistical tie with their base models in most cases and only win in a small number of cases.

We similarly observe limited improvements overall with constrained decoding (Appendix D.1). When we aggregate the results over all (model pair, textual medical knowledge QA dataset) combinations, medical LLMs achieve win/tie/loss rates of 16.9%/68.5%/14.6% in the zero-shot setting and 11.2%/74.2%/14.6% in the 3-shot setting (Table D1). While the aggregate loss rates are generally lower with constrained decoding, the majority of cases still result in a tie, with similar aggregate win and loss rates. Meanwhile, we observe that some medical LLMs show larger improvements with constrained decoding. For example, when switching from greedy to constrained decoding, the zero-shot win/tie/loss rates for MEDI TRON-70B change from 0%/61.5%/38.5% to 30.8%/46.2%/23.1%, showing a substantial increase in the win rate. However, the results are mixed, as some other models (e.g., CLINICAL-CAMEL-70B, OPENBIO LLM-70B) perform worse with constrained decoding.

*In summary, these results show that after appropriately accounting for prompt sensitivity and statistical uncertainty, medical LLMs trained via DAPT show limited improvements in zero-/few-shot prompting performance over their general-domain base models, on textual QA tasks focused on evaluating medical knowledge.*

#### 4.1.2 EVALUATION OF MEDICAL LLMs ON TEXTUAL CLINICAL NOTE QA

In Figures 5(a) and (b), we show the absolute and relative exact-match accuracies achieved by the medical and general-domain LLMs on the textual clinical note QA datasets, from zero-shot and 3-shot prompting, respectively. For the CASI and MIMIC-III sense disambiguation datasets, we also show the absolute and relative *macro* exact-match accuracies and F1 scores—averaged over clinical acronyms—in Figure 6, as the distribution of clinical acronyms in these datasets is highly imbalanced (Adams et al., 2020). In Table 4, we show the win, tie, and loss rates (%) of the medical LLMs, where win rate refers to the proportion of QA datasets where a medical model shows a statistically significant improvement over its base model. As described in Section 3.1, we exclude the 3-shot results for the EHRNoteQA and i2b2 datasets, as a clinical note from even a single QA pair from these datasets on average already fills the context window for most models. Additionally, we exclude the zero-shot results on these datasets for MEDI TRON-7B (and its base model LLAMA-2-7B), as its small context window size of 2k tokens is insufficient even in the zero-shot setting.

In contrast to the zero-shot results on textual medical knowledge QA tasks (Figure 4), the extent of zero-shot performance improvement achieved by the medical LLMs varies more significantly across different model pairs and clinical note QA tasks (Figure 5(a)). In particular, the results vary the most on the four i2b2 datasets, where MED42-v1-70B and CLINICAL-CAMEL-70B (orange) show large improvements (around 20+% in absolute terms), while MEDI TRON-70B (orange), BIOMISTRAL-7B (purple), and BIOMEDGPT-LM-7B (brown) tend to perform worse than their general-domain counterparts. In part, such variability across datasets results from significant differences in the overall syntax, length, and format of the clinical notes provided as context. For the i2b2 datasets, the clinical notes are provided in full with minimal preprocessing, while other datasets often only include short snippets with just a few sentences extracted from the full note (e.g., MedNLI, CASI, MIMIC-III) or apply more extensive preprocessing (e.g., EHRNoteQA).

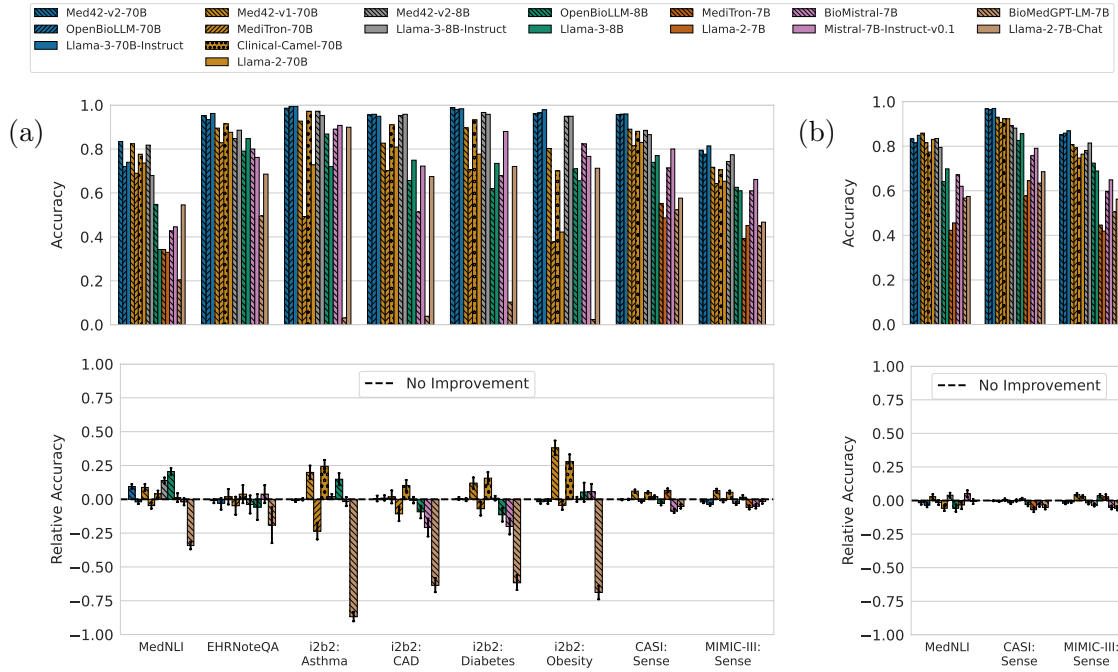


Figure 5: After independently selecting the best prompt format and examples for each model, medical LLMs (textured bars) fail to consistently improve over their base models (solid bars) on textual clinical note QA tasks, in both (a) zero-shot and (b) 3-shot settings. In the 3-shot setting, we exclude the results on the EHRNoteQA and i2b2 datasets given the context window limitations (Section 3.1). In each panel, the top row shows the absolute exact-match accuracies on the test set, and the bottom row shows the relative exact-match accuracies along with 95% confidence intervals derived via bootstrapping on the test set (Section 3). Here, model predictions are generated via greedy decoding. Improvements are also limited with constrained decoding (Figure D2).

Meanwhile, BIOMEDGPT-LM-7B (brown) generally fails to output an appropriate response on these datasets even after performing model-specific prompt selection as in Section 3.1, often refusing to produce an answer or generating irrelevant text completions. We note that such behavior is partially attributable to the lack of details on the recommended prompting setup for BIOMEDGPT-LM-7B (Appendix C.1). BIOMEDGPT-LM-7B does achieve higher accuracy upon constraining its output vocabulary (i.e., constrained decoding), albeit with limited performance improvements over its base model (Figure D2).

In aggregate, we find that the medical models do not consistently improve over their base models in the zero-shot setting (Figure 5(a)). In fact, **only 3 out of 10 medical LLMs—MED42-v1-70B, CLINICAL-CAMEL-70B, and MED42-v2-8B—win more than they lose to their base models in the zero-shot setting** (Table 4). Across all (model pair, textual clinical note QA dataset) combinations, the medical LLMs achieve zero-shot win/tie/loss rates of 28.0%/36.0%/36.0%. Meanwhile, MED42-v1-70B and CLINICAL-CAMEL-70B show substantial improvements in the zero-shot setting, respectively achieving win rates of 75.0% and 87.5%, and both achieving a loss rate of 0%. The two models also tend to show strong

Table 4: The zero-shot and 3-shot win, tie, and loss rates (%) of all medical LLMs on textual clinical note QA, after independently optimizing the prompt for each model. For each medical model, we boldface the win rate if it wins more than it loses to its general-domain base model, and vice versa. Here, we show the results when model predictions are generated via greedy decoding. The results for constrained decoding are shown in Table D2.

Model	Zero-Shot			3-Shot		
	Win	Tie	Loss	Win	Tie	Loss
MED42-V2-70B	12.5	62.5	<b>25.0</b>	0	33.3	<b>66.7</b>
OPENBIO-LLM-70B	0	75.0	<b>25.0</b>	0	0	<b>100.0</b>
MED42-V1-70B	<b>75.0</b>	25.0	0	<b>66.7</b>	33.3	0
MEDI-TRON-70B	0	25.0	<b>75.0</b>	33.3	33.3	33.3
CLINICAL-CAMEL-70B	<b>87.5</b>	12.5	0	0	33.3	<b>66.7</b>
MED42-V2-8B	<b>37.5</b>	50.0	12.5	<b>66.7</b>	0	33.3
OPENBIO-LLM-8B	25.0	37.5	<b>37.5</b>	33.3	0	<b>66.7</b>
MEDI-TRON-7B	33.3	33.3	33.3	33.3	0	<b>66.7</b>
BIO-MISTRAL-7B	12.5	37.5	<b>50.0</b>	33.3	0	<b>66.7</b>
BIO-MEDGPT-LM-7B	0	0	<b>100.0</b>	0	33.3	<b>66.7</b>
<b>Aggregate</b>	28.0	36.0	<b>36.0</b>	26.7	16.7	<b>56.7</b>

performance on the i2b2 datasets, which, unlike other datasets, are based on minimally pre-processed, full-length clinical notes. A notable difference between these two models and others is that their corresponding medical adaptation corpora include datasets beyond PubMed articles (e.g., medical knowledge QA datasets), often in *conversational formats* (Table 2). Given that both were adapted from LLAMA-2-70B, which has not been instruction-tuned and thus may not reliably generate an appropriate response in the zero-shot setting, we note that the perceived performance improvements may be overestimated in this setting.

In the 3-shot setting, where even non-instruction-tuned LLMs generally output a relevant response in the correct format, the majority of medical LLMs show little to no improvement over their base models, with the 95% confidence intervals in relative exact-match accuracy crossing or lying below zero (Figure 5(b)). **Only 2 out of 10 medical LLMs**—MED42-V1-70B and MED42-V2-8B—**show significant improvements in the 3-shot setting** (Table 4). When aggregated across all (model pair, textual clinical note QA dataset) combinations, the medical LLMs achieve 3-shot win/tie/loss rates of 26.7%/16.7%/56.7%.

On the CASI and MIMIC-III sense disambiguation datasets, the medical LLMs fail to show significant improvements over their base models *even after accounting for the imbalance in the distribution of clinical acronyms*, in both zero-shot (Figure 6(a)) and 3-shot (Figure 6(b)) settings. On the CASI dataset, only 3 out of 10 medical LLMs show improvement in the zero-shot setting in terms of macro-average accuracy, and none of the medical LLMs show improvement in the 3-shot setting. In terms of macro-average F1 score, only 2 out of 10 medical LLMs show improvement in the zero-shot setting, while none of the medical LLMs show improvement in the 3-shot setting. On the MIMIC-III dataset, only 2 out of 10 medical LLMs show improvement in the zero-shot setting in terms of each metric, and only 3 out of 10 medical LLMs show improvement in the 3-shot setting in terms of each metric.

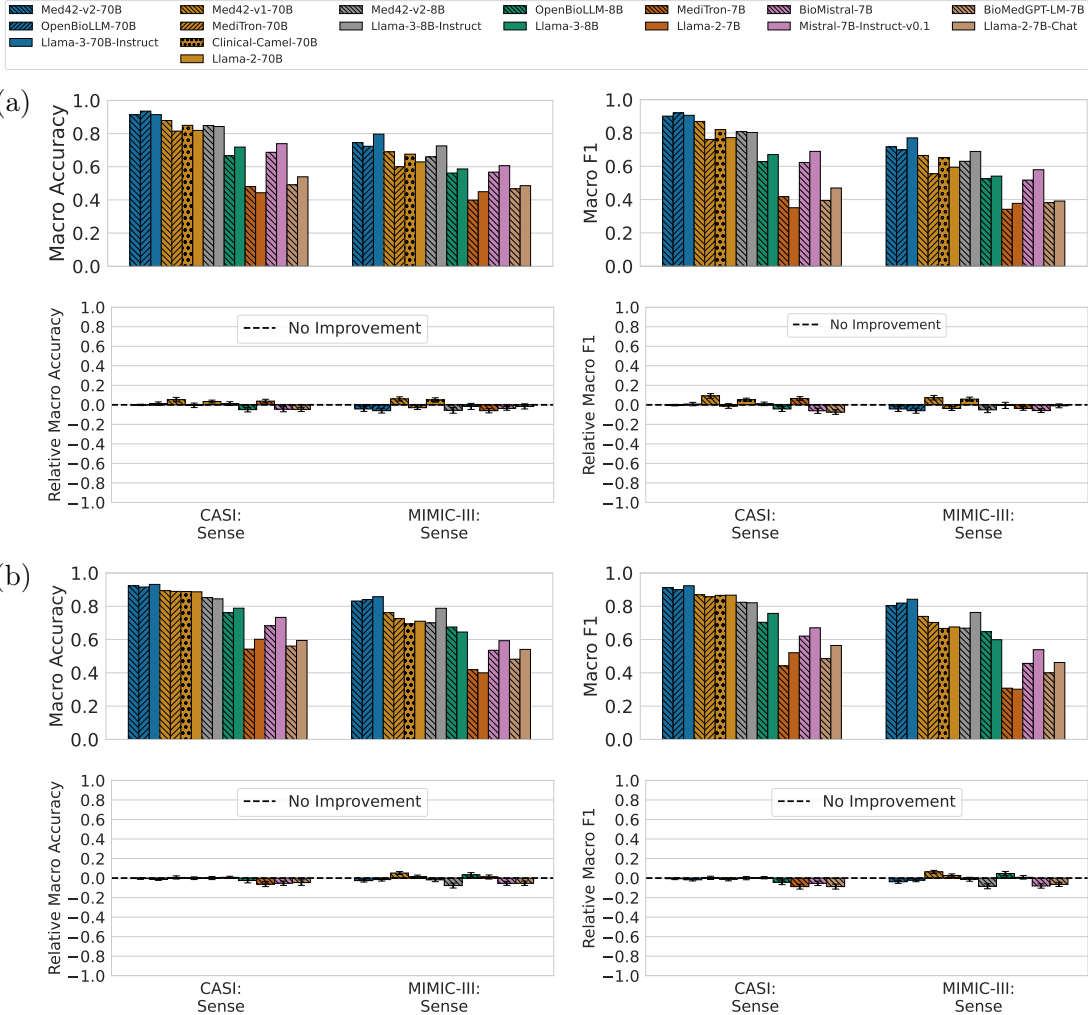


Figure 6: Even after accounting for the imbalance in the distribution of clinical acronyms in the CASI and MIMIC-III datasets, medical LLMs (textured bars) fail to consistently improve over their base models (solid bars), in both (a) zero-shot and (b) 3-shot settings. We show the results when the prompts are optimized for each model independently. In each panel, the top row shows the absolute macro exact-match accuracies and F1 scores—averaged over clinical acronyms—on the test set, and the bottom row shows the relative macro exact-match accuracies and F1 scores along with 95% confidence intervals derived via bootstrapping on the test set (Section 3). Here, model predictions are generated via greedy decoding. Improvements are also limited with constrained decoding (Figure D3).

We similarly observe limited improvements overall with constrained decoding (Appendix D.2). When we aggregate the results over all (model pair, textual clinical note QA dataset) combinations, medical LLMs achieve win/tie/loss rates of 34.7%/37.3%/28.0% in the zero-shot setting and 33.3%/23.3%/43.3% in the 3-shot setting (Table D2). While the aggregate loss rates are generally lower with constrained decoding, the win rates are roughly equivalent to the loss rates modulo the statistical ties. We also see limited improvements

in terms of macro-average accuracy and F1 score on the CASI and MIMIC-III datasets (Figure D3). Meanwhile, as for the textual medical knowledge QA tasks, some medical LLMs show larger improvements with constrained decoding. For example, when switching from greedy to constrained decoding, we observe that the zero-shot win/tie/loss rates for BIOMEDGPT-LM-7B change from 0%/0%/100.0% to 50.0%/12.5%/37.5%, showing a substantial increase in the win rate. However, the results are again mixed, as some other models (e.g., MEDI TRON-7B and BIOMISTRAL-7B) perform worse with constrained decoding.

*In summary, these results demonstrate that on textual QA tasks based on real-world clinical notes, medical LLMs trained via DAPT show limited improvements in zero-/few-shot prompting performance over their general-domain counterparts after appropriately accounting for prompt sensitivity and statistical uncertainty.*

#### 4.1.3 EVALUATION OF MEDICAL VLMs ON VISUAL MEDICAL QA

In Figures 7(a) and (b), we show the absolute and relative exact-match accuracies achieved by the medical and general-domain VLMs on the visual medical QA datasets, from zero-shot and 3-shot prompting, respectively. Table 5 shows the win, tie, and loss rates (%) of the medical VLMs, where win rate refers to the proportion of visual medical QA datasets where a medical model shows a statistically significant improvement over its base model. We note that both LLAVA-MED-7B and its base model LLAVA-v0-7B were not pretrained to handle multi-image inputs and may not perform better with more in-context examples.

In both zero-shot and 3-shot settings, we find that the absolute exact-match accuracies are mostly similar between each model pair on VQA-RAD, PathVQA, and SLAKE (Figure 7). On the three datasets, the absolute accuracies tend to be higher for all models in the 3-shot vs. the zero-shot setting, but the pairwise differences remain similarly small in both settings. For MMMU-Medical on the other hand, we see that the extent of performance improvement (or lack thereof) varies significantly across the two model pairs and datasets, and that the absolute exact-match accuracies do not exhibit an increasing trend going from zero-shot to 3-shot prompting. For example, when comparing the absolute accuracies between each VLM pair in the zero-shot setting, LLAVA-MED-7B generally performs significantly worse than LLAVA-v0-7B (**light green**), while MED-FLAMINGO-9B generally performs significantly better than OPEN-FLAMINGO-9B (**cyan**) across all subjects in MMMU-Medical. Meanwhile, on the MMMU-Medical datasets, the 95% confidence intervals in relative exact-match accuracy almost always cross zero, indicating that the observed differences are *not* statistically significant (bottom rows of Figure 7(a) and (b)). We note that the confidence intervals are much wider on MMMU-Medical than on the other datasets, as the test sets only include 25 QA examples per subject in MMMU-Medical (Table A1).

When we aggregate the results across all model pairs and visual medical QA datasets while accounting for such statistical uncertainty, we find that the medical VLMs only achieve win/tie/loss rates of 6.3%/75.0%/18.8% in the zero-shot setting and 6.3%/81.3%/12.5% in the 3-shot setting (Table 5). In fact, we find that both LLAVA-MED-7B and MED-FLAMINGO-9B are **virtually indistinguishable from their base models in terms of performance**: LLAVA-MED-7B achieves win/tie/loss rates of 12.5%/62.5%/25.0% in both zero-shot and 3-shot settings, while MED-FLAMINGO-9B achieves win/tie/loss rates of 0%/87.5%/12.5% in the zero-shot setting and 0%/100%/0% in the 3-shot setting.

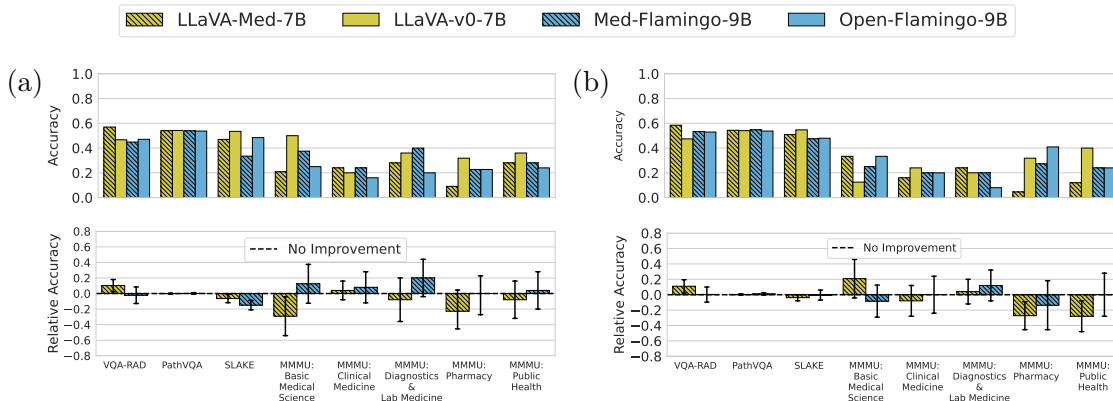


Figure 7: After independently selecting the best prompt format and examples for each model, medical VLMs (textured bars) fail to consistently improve over their base models (solid bars) on visual medical QA tasks, in both (a) zero-shot and (b) 3-shot settings. In each panel, the top row shows the absolute exact-match accuracies on the test set, and the bottom row shows the relative exact-match accuracies along with 95% confidence intervals derived via bootstrapping on the test set (Section 3). Here, model predictions are generated via greedy decoding. Improvements are also limited with constrained decoding (Figure D4).

Table 5: The zero-shot and 3-shot win, tie, and loss rates (%) of all medical VLMs on visual medical QA, after independently optimizing the prompt for each model. For each medical model, we boldface the win rate if it wins more than it loses to its general-domain base model, and vice versa. Here, we show the results when model predictions are generated via greedy decoding. The results for constrained decoding are shown in Table D3.

Model	Zero-Shot			3-Shot		
	Win	Tie	Loss	Win	Tie	Loss
LLAVA-MED-7B	12.5	62.5	<b>25.0</b>	12.5	62.5	<b>25.0</b>
MED-FLAMINGO-9B	0	87.5	<b>12.5</b>	0	100.0	0
Aggregate	6.3	75.0	<b>18.8</b>	6.3	81.3	<b>12.5</b>

We observe that these conclusions also hold when the model predictions are generated via constrained decoding (Appendix D.3). The medical VLMs almost always reach a tie with their base models in both zero-shot and 3-shot settings, with the 95% confidence intervals in relative exact-match accuracy crossing zero (Figure D4). Collectively, the medical VLMs achieve win/tie/loss rates of 6.3%/87.5%/6.3% in the zero-shot setting and 0%/93.8%/6.3% in the 3-shot setting (Table D3). In fact, **no medical VLM shows improvement over its general-domain base model, regardless of the decoding strategy.**

*In summary, these results show that after appropriately accounting for prompt sensitivity and statistical uncertainty, medical VLMs trained via DAPT show limited improvements in zero-/few-shot prompting performance over their general-domain counterparts, on visual medical QA tasks spanning various medical imaging modalities (e.g., pathology, radiology).*

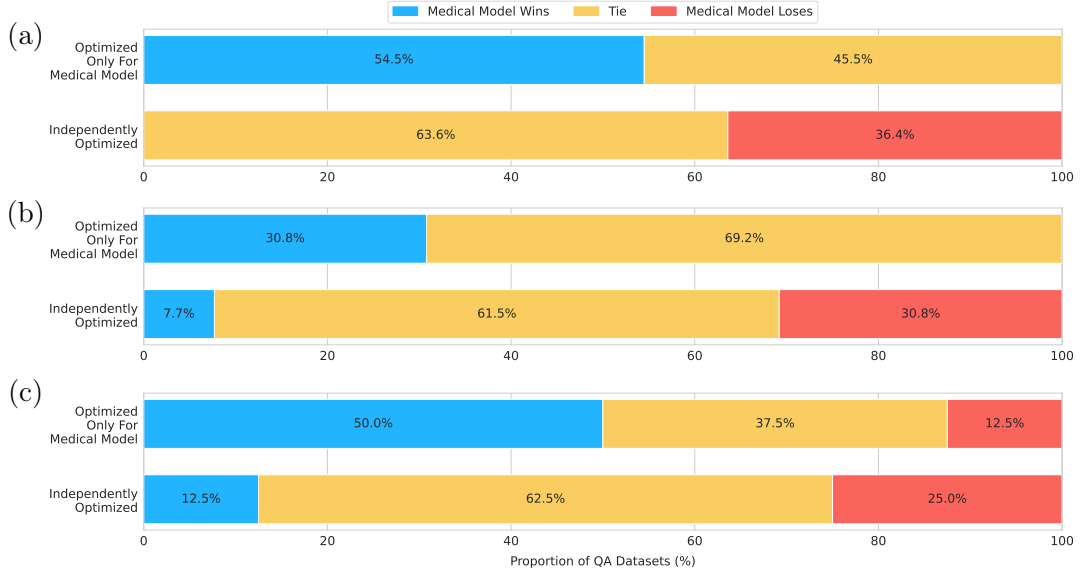


Figure 8: Using a single, fixed prompt only optimized for the medical model can overestimate the performance improvements from medical DAPT: (a) CLINICAL-CAMEL-70B, (b) OPENBIO-LLM-8B, (c) LLAVA-MED-7B. “Optimized Only For Medical Model” refers to the setting where we perform model-specific prompt selection (Section 3.1) only for the medical model and use the selected prompt for both models in each pair. “Independently Optimized” refers to the setting where we separately perform model-specific prompt selection for each model in a given pair. For CLINICAL-CAMEL-70B and OPENBIO-LLM-8B, we show the 3-shot win/tie/loss rates (%) on the textual medical knowledge QA tasks (trends are similar for the textual clinical note QA tasks; see Section 4.2.3). For LLAVA-MED-7B, we show the 3-shot win/tie/loss rates (%) on all visual medical QA tasks.

## 4.2 Overlooking Prompt Sensitivity and Statistical Uncertainty May Overestimate the Performance Benefits from Medical DAPT

Based on our findings in Section 4.1, we further investigate whether the conclusions differ if the same prompt is used for each pair of medical and general-domain models. In particular, we consider whether selecting a prompt only for the medical model, following Section 3.1, and using it for the corresponding general-domain base model can widen the performance gap between each pair. We also assess whether this gap becomes amplified when models are compared without accounting for statistical uncertainty, which is often observed in practice. More concretely, we evaluate how the win/tie/loss rates (%) of the medical models change across all QA tasks, as we vary the following aspects of the experimental setup:

1. select prompts for each model independently vs. only based on the medical model;
2. determine the winner for each model pair based on statistical testing (allowing for ties) vs. comparing only based on absolute accuracy.

Note that when comparing each model pair based on raw absolute accuracy, there are no ties, as the real-valued absolute accuracies are rarely identical.

Overall, we find that the perceived performance benefits from medical DAPT can be significantly overestimated without appropriately accounting for prompt sensitivity and statistical uncertainty in the results. We consistently observe this across all LLM/VLM pairs and medical QA tasks. Using specific model pairs as examples, we illustrate our findings regarding each aspect in Sections 4.2.1–4.2.2, and discuss the aggregate result across all model pairs and QA datasets in Section 4.2.3.

#### 4.2.1 SELECTING THE “RIGHT” PROMPT INDEPENDENTLY IS CRUCIAL FOR A FAIR COMPARISON BETWEEN MODELS

In Figure 8, we show how the win, tie, and loss rates (%) change when we optimize the prompt only for the medical model, using CLINICAL-CAMEL-70B, OPENBIO-LLM-8B, and LLAVA-MED-7B as illustrative examples. For CLINICAL-CAMEL-70B and OPENBIO-LLM-8B, we show the 3-shot results on the textual medical knowledge QA datasets (see Section 4.2.3 for discussion of results on textual clinical note QA, which are similar). For LLAVA-MED-7B, we show the 3-shot results on all visual medical QA datasets. We note that the results here are shown *with* statistical testing, i.e., the win/tie/loss rates are calculated based on the 95% bootstrapping confidence intervals, as described in Section 3.

In all three cases, we observe that when we optimize the prompt only for the medical model, the win rates increase significantly and the loss rates decrease significantly. For example, we find that the win rate for CLINICAL-CAMEL-70B increases from 0% to 54.5% while its loss rate decreases from 36.4% to 0% under this setting, completely reversing the conclusion about CLINICAL-CAMEL-70B (Figure 8(a)). We also observe that such trends exist regardless of model scale: across both 70B-parameter and 7/8B-parameter models, the results are highly sensitive to the choice of prompt format and few-shot examples.

Notably, we find that such differences in performance can result from seemingly insignificant differences in the prompt. Below, we show the prompt formats optimized for CLINICAL-CAMEL-70B and LLAMA-2-70B on MMLU (Clinical Knowledge):

##### CLINICAL-CAMEL-70B vs. LLAMA-2-70B on MMLU (Clinical Knowledge)

###### Prompt Format Optimized for CLINICAL-CAMEL-70B:

\*\*Question\*\*= Glycolysis is the name given to the pathway involving the conversion of:

- (A) glycogen to glucose-1-phosphate.
- (B) glycogen or glucose to fructose.
- (C) glycogen or glucose to pyruvate or lactate.
- (D) glycogen or glucose to pyruvate or acetyl CoA.

\*\*Answer\*\*=

###### Prompt Format Optimized for LLAMA-2-70B:

### Question: Glycolysis is the name given to the pathway involving the conversion of:

- (A) glycogen to glucose-1-phosphate.
- (B) glycogen or glucose to fructose.
- (C) glycogen or glucose to pyruvate or lactate.

(D) glycogen or glucose to pyruvate or acetyl CoA.

### Answer:

We find that the main difference in the prompt, modulo the selected few-shot examples, lies on how the question and answer headers are formatted, with the overall semantics of the overall prompt remaining completely intact. We also note that the task instruction provided to CLINICAL-CAMEL-70B and LLAMA-2-70B is also identical: “The following is a multiple-choice question about medical knowledge. Answer the question by choosing one of the options from A to D.” These results are consistent with the conclusions of prior works that demonstrate that the behavior of LLMs/VLMs are highly sensitive to the specifics of the input prompt (Jiang et al., 2020; Zhao et al., 2021; Sclar et al., 2024), including works specifically focused on clinical tasks (Ceballos-Arroyo et al., 2024).

*Our findings suggest that selecting the “right” prompt format and few-shot examples for each model separately is crucial for a fair comparison in the zero-/few-shot prompting regime.*

#### 4.2.2 IGNORING STATISTICAL UNCERTAINTY CAN LEAD TO MISLEADING CONCLUSIONS ABOUT PERFORMANCE IMPROVEMENTS FROM MEDICAL DAPT

In Figure 9, we show how the win, tie, loss rates (%) change when we remove statistical testing, comparing the performances of each model pair solely based on raw absolute accuracy. As in Section 4.2.1, we show the 3-shot results for CLINICAL-CAMEL-70B and OPENBIO-LLM-8B on the textual medical knowledge QA datasets, and the 3-shot results for LLAVA-MED-7B on all visual medical QA datasets. We note that the results here are shown *after* performing model-specific prompt selection for each model independently.

In all three cases, we overall observe that due to the absence of ties when comparing based on raw absolute accuracy, both the win and loss rates can become overestimated. In particular, we observe that the win rate for LLAVA-MED-7B in the 3-shot setting increases from 12.5% to 62.5%, reversing the conclusions about its improvement over its base model LLAVA-v0-7B (Figure 9(c)). For CLINICAL-CAMEL-70B and OPENBIO-LLM-8B, we find that while both models lose more than they win against their base models with or without statistical testing, the failure to account for statistical ties also leads to an overly pessimistic conclusion. In fact, with statistical testing, both models reach a tie in 60+% of QA datasets when we account for statistical uncertainty (Figures 9(a) and (b)), which is almost entirely ignored when comparing based on raw accuracy. Accounting for statistical uncertainty allows one to more accurately conclude that all three models reach a statistical tie in most cases, with little to no statistically significant improvements in performance.

*These findings suggest that in order to draw reliable conclusions about the performance benefits from medical DAPT, it is essential to take statistical uncertainty into consideration.*

#### 4.2.3 IGNORING PROMPT SENSITIVITY AND STATISTICAL UNCERTAINTY CAN OVERESTIMATE THE PERFORMANCE BENEFITS FROM MEDICAL DAPT

Based on the findings discussed in Sections 4.2.1–4.2.2, we investigate how the lack of (i) independent prompt selection and (ii) statistical testing can change the broader conclusions about the effectiveness of medical DAPT in improving zero-/few-shot prompting performance. In total, we consider four different scenarios, resulting from the inclusion or exclu-

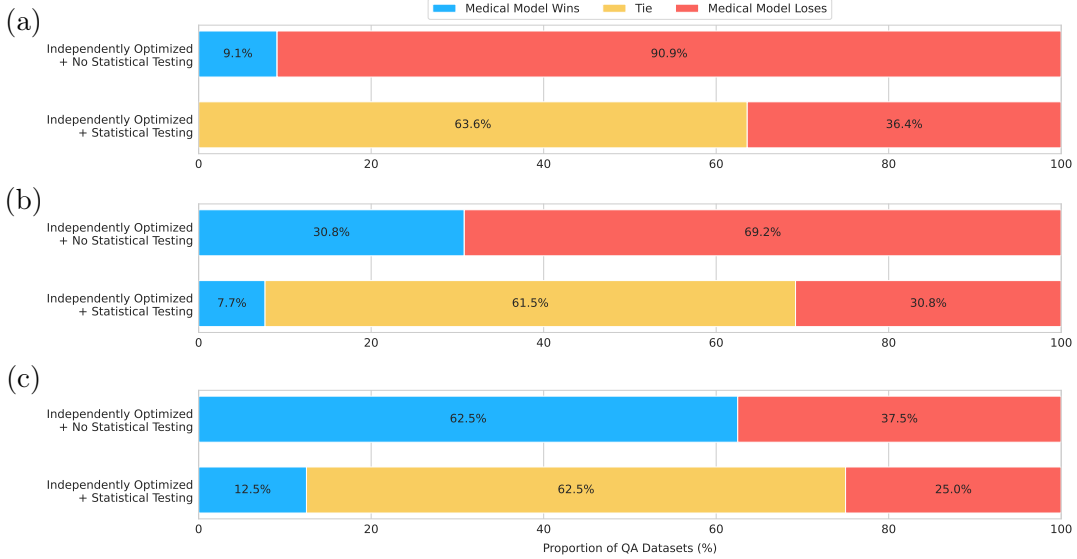


Figure 9: Ignoring statistical uncertainty in model comparison can lead to overly optimistic or pessimistic conclusions about the performance benefits from medical DAPT: (a) CLINICAL-CAMEL-70B, (b) OPENBIO-LLM-8B, (c) LLAVA-MED-7B. Here, we show the results when we separately perform model-specific prompt selection for each model in a given pair (“Independently Optimized”). “No Statistical Testing” refers to the setting where we compare models based on raw absolute accuracy. “Statistical Testing” refers to the setting where we compare models based on the 95% confidence intervals in relative accuracy. For CLINICAL-CAMEL-70B and OPENBIO-LLM-8B, we show the 3-shot win/tie/loss rates (%) on the textual medical knowledge QA tasks (trends are similar for the textual clinical note QA tasks; see Section 4.2.3). For LLAVA-MED-7B, we show the 3-shot win/tie/loss rates (%) on all visual medical QA tasks. *Without statistical testing, both win and loss rates can be overestimated due to the failure to account for statistical ties.*

sion of these two aspects of the experimental setup. We aggregate all of the zero-shot and 3-shot results on textual medical knowledge QA, textual clinical note QA, and visual QA.

When we aggregate the results over all (model pair, QA dataset) combinations, we find that for both LLMs and VLMs, the performance improvement from medical DAPT can be substantially overestimated when (i) the prompt is only tailored to the medical model; and (ii) the models are compared only based on their absolute accuracies (Figure 10). For example, the aggregate zero-shot win rate substantially increases from 9.0% to 74.2% on textual medical knowledge QA, 28.0% to 60.0% on textual clinical note QA, and 6.3% to 62.5% on visual medical QA, when only performing prompt selection for the medical model and comparing based on raw absolute accuracy. We see a similar trend in the win/tie/loss rates when the model predictions are generated via constrained decoding (Figure D5).

*In summary, these results highlight the importance of accounting for LLM/VLM sensitivity to the prompting details (Section 4.2.1) and statistical uncertainty (Section 4.2.2), in order to draw reliable conclusions about the effectiveness of medical DAPT (Section 4.2.3).*

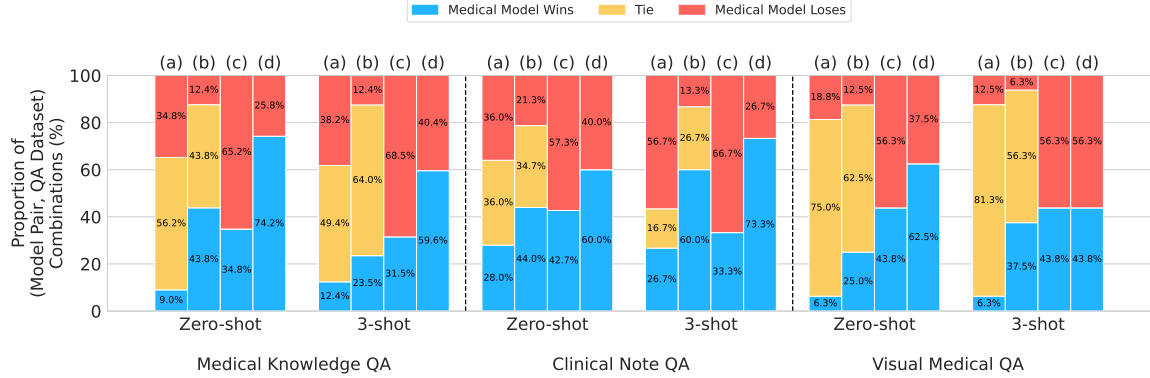


Figure 10: Optimizing the prompt for only the medical model and comparing models without accounting for statistical uncertainty can overestimate the performance improvements from medical DAPT. We show the win/tie/loss rates (%) of the medical models across all (model pair, QA dataset) combinations, when (a) optimizing the prompt for each model, with statistical testing; (b) optimizing the prompt only for the medical model, with statistical testing; (c) optimizing the prompt for each model, without statistical testing; and (d) optimizing the prompt only for the medical model, without statistical testing. We show the results for greedy decoding. The results for constrained decoding are similar (Figure D5).

## 5 Supervised Fine-Tuning (SFT) Evaluation Results

We summarize the main findings from the SFT experiments outlined in Section 3.2. Overall, we find that after SFT, medical LLMs *do* show statistically significant improvements on the textual medical knowledge QA datasets (Section 5.1) but not on the clinical note QA datasets (Section 5.2), while medical VLMs do not show consistent improvements on the visual medical QA datasets (Section 5.3).

### 5.1 Evaluation of Medical LLMs on Textual Medical Knowledge QA

In Figure 11(a), we show the absolute and relative exact-match accuracies achieved by the medical and general-domain LLMs on the textual medical knowledge QA datasets, after fine-tuning each model. In Table 6 (left), we also show the win, tie, and loss rates (%) of the medical LLMs on these datasets. As discussed in Section 3.2, we do not evaluate on the MMLU-Medical datasets, which only have 5 examples in the training set per subject (Table A1). We also exclude the results for the MED42 models, since they have already been trained on all medical knowledge QA datasets via medical DAPT (Table 2).

Overall, we find that **medical LLMs *do* consistently improve over their general-domain base models in the SFT regime**. All medical LLMs generally perform better than their base models in absolute terms, albeit with marginal improvements (on average, 1.6% improvement in absolute accuracy) (top row of Figure 11(a)). In most cases, these improvements are nonetheless statistically significant, with the 95% confidence intervals in relative accuracy lying above zero (bottom row of Figure 11(a)). In fact, all medical LLMs achieve loss rates of 0%, with 5 out of 7 models achieving win rates of 50+% (Table 6, left). Even BIOMEDGPT-LM-7B (brown), which significantly underperforms its

Table 6: The win, tie, and loss rates (%) of all medical LLMs on textual medical knowledge QA (left) and textual clinical note QA (right), after fine-tuning them on the training set of each QA dataset. For each medical model, we boldface the win rate if it wins more than it loses to its general-domain base model, and vice versa. We exclude the results for the MED42 models on the textual medical knowledge QA datasets, as they have already been trained on all of those datasets during medical DAPT.

Model	Medical Knowledge			Clinical Note		
	Win	Tie	Loss	Win	Tie	Loss
MED42-v2-70B	-	-	-	<b>37.5</b>	62.5	0
OPENBIOILLM-70B	<b>50.0</b>	50.0	0	<b>12.5</b>	87.5	0
MED42-v1-70B	-	-	-	0	100.0	0
MEDI TRON-70B	<b>75.0</b>	25.0	0	0	100.0	0
CLINICAL-CAMEL-70B	0	100.0	0	0	100.0	0
MED42-v2-8B	-	-	-	12.5	75.0	12.5
OPENBIOILLM-8B	<b>25.0</b>	75.0	0	0	100.0	0
MEDI TRON-7B	<b>75.0</b>	25.0	0	0	100.0	0
BIO MISTRAL-7B	<b>50.0</b>	50.0	0	0	100.0	0
BIO MEDGPT-LM-7B	<b>75.0</b>	25.0	0	0	87.5	<b>12.5</b>
<b>Aggregate</b>	<b>53.8</b>	46.2	0	<b>6.7</b>	90.7	2.7

base model LLAMA-2-7B-CHAT in the zero-/few-shot prompting regime (Sections 4.1–4.2), achieves a win rate of 75.0%. We also find that medical models based on more recent general-domain base models (e.g., OPENBIOILLM-70B and OPENBIOILLM-8B, based on LLAMA-3) tend to show lower win rates than the other medical models based on older general-domain base models (e.g., MEDI TRON and BIO MEDGPT-LM, based on LLAMA-2).

*Together with our findings from Sections 4.1–4.2, these results suggest that additional training on biomedical text indeed provides a better initialization of the parameters for downstream fine-tuning on textual medical knowledge QA tasks, while the off-the-shelf capabilities of medically adapted LLMs are overall no better than those of their base models.*

## 5.2 Evaluation of Medical LLMs on Textual Clinical Note QA

In Figure 11(c), we show the absolute and relative exact-match accuracies achieved by the medical and general-domain LLMs on the textual clinical note QA datasets, after fine-tuning each model. For the CASI and MIMIC-III sense disambiguation datasets, we also show the absolute and relative macro exact-match accuracies and F1 scores—averaged over clinical acronyms—in Figure 12 to account for the imbalance in the acronym distribution (Section 4.1.2). In Table 6 (right), we also show the win, tie, and loss rates (%) of the medical LLMs on these datasets. As in the zero-/few-shot prompting evaluations discussed in Section 4.1.2, we exclude the results for MEDI TRON-7B (and its base model LLAMA-2-7B) on the EHRNoteQA and i2b2 datasets, as its small context window size of 2k tokens is insufficient for handling the full-length clinical notes in these datasets.

Across all model pairs and datasets, we find that the **fine-tuning performances of the medical LLMs and those of their base models are nearly indistinguishable**

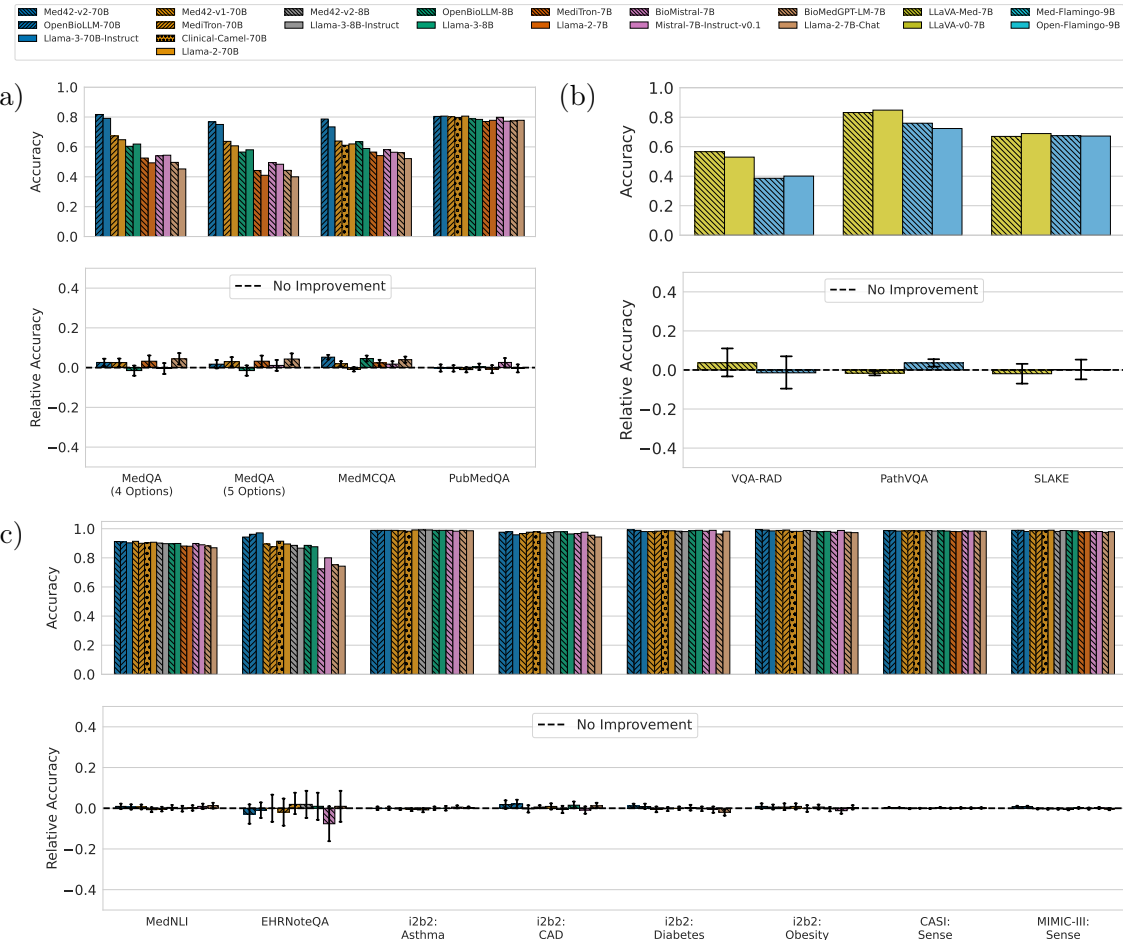


Figure 11: Absolute and relative accuracies of (a) all LLMs on textual medical knowledge QA, (b) all VLMs on visual medical QA, and (c) all LLMs on textual clinical note QA, after SFT on each task. *Overall, medical LLMs do show improvement in SFT performance on the textual medical knowledge QA datasets, but not on the textual clinical note QA datasets. Medical VLMs do not show significant improvements on the visual medical QA datasets.*

(Figure 11(c)). In Figure 12, we make similar observations on the CASI and MIMIC-III sense disambiguation datasets even after accounting for the imbalance in the clinical acronym distribution. In Table 6 (right), we find that across all (model pair, textual clinical note QA dataset) combinations, 90.7% of cases result in a statistical tie, with the medical models winning against their base models in only 6.7% of cases. In fact, **7 out of 10 medical LLMs are indistinguishable from their base models in terms of the win/tie/loss rates**. Meanwhile, we observe that while the LLMs do not consistently perform well *off-the-shelf* on clinical note QA (Section 4.1.2), both medical and general-domain models uniformly show strong performance after being fine-tuned for each task, across all model scales.

*These results suggest that additional training on biomedical text data, as commonly done for the medical LLMs that we evaluate (Table 2), is not particularly beneficial for improving downstream supervised fine-tuning performance on QA tasks involving clinical notes.*

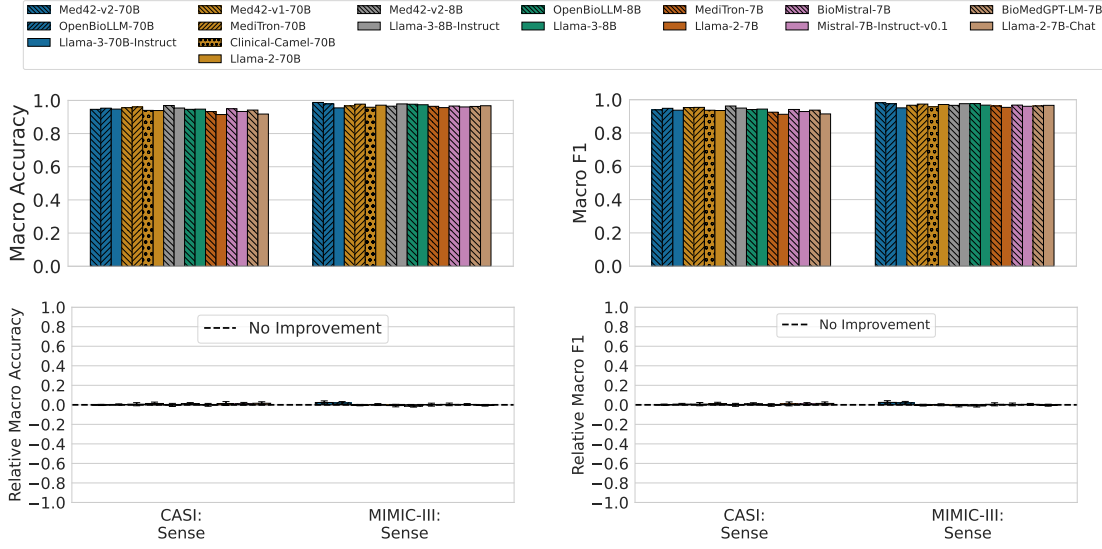


Figure 12: Even after accounting for the imbalance in the distribution of clinical acronyms in the CASI and MIMIC-III sense disambiguation datasets, medical LLMs fail to consistently improve over their base models, after SFT. In each panel, the top row shows the absolute macro exact-match accuracies and F1 scores—averaged over clinical acronyms—on the test set, and the bottom row shows the relative macro exact-match accuracies and F1 scores along with 95% confidence intervals derived via bootstrapping on the test set (Section 3).

Table 7: The win, tie, and loss rates (%) of all medical VLMs on visual medical QA, after fine-tuning them on the training set of each QA dataset. For each medical model, we boldface the win rate if it wins more than it loses to its general-domain base model, and vice versa.

Model	Visual Medical QA		
	Win	Tie	Loss
LLAVA-MED-7B	0	66.7	33.3
MED-FLAMINGO-9B	<b>33.3</b>	66.7	0
Aggregate	16.7	66.7	16.7

### 5.3 Evaluation of Medical VLMs on Visual Medical QA

In Figure 11(b), we show the absolute and relative exact-match accuracies achieved by the medical and general-domain VLMs on the visual medical QA datasets, after fine-tuning each model. In Table 7, we also show the win, tie, and loss rates (%) of the medical VLMs on these datasets. As discussed in Section 3.2, we do not evaluate on the MMMU-Medical datasets, which only have 5 examples in the training set per subject (Table A1).

Overall, **medical VLMs do not consistently improve over their general-domain base models in the SFT regime**. We observe that LLAVA-MED-7B (light green) shows no statistically significant improvements over its base model, while MED-FLAMINGO-9B (cyan) shows improvement on PathVQA (+3.5% in raw accuracy) but reaches a tie in others (Figure 11(b)). When we aggregate the results across all (model pair, visual medical QA

dataset) combinations, the medical VLMs achieve win/tie/loss rates of 16.7%/66.7%/16.7% (Table 7), indicating limited collective improvement. Meanwhile, given that these conclusions are based on a relatively small number of models (only 2) and datasets (only 3), we note that the generalizability of this finding may be limited.

*In summary, the results in Sections 5.1–5.3 show that in the SFT regime, medical LLMs show improvements on textual QA tasks focused on assessing medical knowledge but not on those based on clinical notes, while medical VLMs generally fail to show statistically significant improvements on the visual medical QA datasets.*

## 6 Discussion and Conclusion

In this work, we investigated the effectiveness of DAPT for training medically specialized LLMs and autoregressive VLMs suitable for various medical (visual) QA tasks. To that end, we compared several pairs of state-of-the-art medical LLMs/VLMs to their general-domain counterparts, whose only differences lie in medical DAPT and are exactly identical in model architecture and scale. Our work differs from prior works by providing direct apples-to-apples comparisons of medical and general-domain base models, while accounting for LLM/VLM sensitivity to prompting details and assessing the statistical significance of the results. We also ensure that our evaluations are comprehensive by (i) comparing the models in both the zero-/few-shot prompting and SFT regimes; and (ii) covering both QA tasks focused on assessing medical knowledge and those based on real-world clinical notes.

In the zero-/few-shot prompting regime, we found that across both model classes and all model scales, the performance benefits from medical DAPT largely disappear when we (i) tailor the prompt format and choice of few-shot examples to each medical and general-domain model separately; and (ii) account for statistical uncertainty in model comparison (Section 4.1). In particular, we found that when we optimize the prompt only for the medical model and compare each model pair based on their absolute accuracies without accounting for uncertainty, the performance improvements from medical DAPT can be significantly overestimated (Section 4.2), potentially leading to unreliable conclusions about the benefits of medical DAPT on zero-/few-shot prompting performance.

In the SFT regime, we found that medical LLMs overall do show statistically significant improvements on textual QA tasks focused on assessing medical knowledge (Section 5.1) but not on clinically relevant QA tasks that based on real-world clinical notes (Section 5.2). For medical VLMs, we found that they overall fail to show significant improvements on the visual medical QA tasks that we consider, which we present with the caveat that our findings are based on a relatively small number of VLMs and datasets (Section 5.3).

Our findings suggest that for state-of-the-art general-domain LLMs and VLMs, the performance benefits from additionally pretraining on medical data from public sources such as PubMed may be limited. In fact, almost all of the medical models used in our evaluation use PubMed as the primary source of pretraining data for medical adaptation (Table 2), while open-source datasets commonly used for pretraining the general-domain base models in the first place (e.g., the Pile (Gao et al., 2020), S2ORC (Lo et al., 2020)) often already include PubMed data. Thus, we emphasize that any claims of improvement due to proposed medical DAPT procedures should be backed up by rigorous head-to-head comparisons against the corresponding general-domain base models.

**Limitations.** First, there is a vast and growing set of papers on applying medical DAPT to various general-domain base models, and we could not hope to compare all publicly available models here. While we selected the models to cover a wide range of general-domain base models and model scales (7B–70B) (Table 2) and included some of the latest models (e.g., OPENBIOLLM and LLAMA-3), it is always possible that some newly released models do in fact yield better zero-/few-shot or SFT performance on medical QA.

Second, we focus in this paper on the narrower task of closed-ended medical QA. In part, this choice reflects the fact that such benchmarks are well-standardized and highly publicized. However, they do not reflect the breadth of possible applications of LLMs and VLMs in medical domains. For instance, Singhal et al. (2023b) show that medical LLMs such as MED-PALM-2 can produce physician-level answers to open-ended consumer health queries; Liu et al. (2022) explore the use of LLMs for generating discharge instructions based on a patient’s health records; and Li et al. (2023b) demonstrate the potential of using LLMs to recommend treatments for patients based on patient-doctor conversations. Some would argue that such tasks are a more realistic application of such models in practice, and it is certainly possible that an analysis like ours would find improved performance on such tasks, though we do not investigate these tasks in the present work.

Third, due to computational constraints, we do not consider full fine-tuning of models for evaluations in the SFT regime. Prior works show that parameter-efficient fine-tuning performance (e.g., LoRA) can be worse than that of full fine-tuning, and that the gap in performance varies significantly across different tasks (Christophe et al., 2024a; Biderman et al., 2024). While our head-to-head comparisons based on parameter-efficient fine-tuning revealed that medical models show limited improvement over their base models across all model scales, the overall conclusions may be different in the full fine-tuning regime.

While we acknowledge the limitations above, we do not believe they detract from the value of this work. We hope that our results call attention to a need for rigorous head-to-head evaluations when making similar claims of improved performance via medical DAPT, whether with other models, on other clinical tasks, or with respect to SFT versus zero-/few-shot prompting performance.

## Acknowledgments and Disclosure of Funding

We gratefully acknowledge DARPA (FA8750-23-2-1015), ONR (N00014-23-1-2368), NSF (IIS2211955), UPMC, Highmark Health, Abridge, Ford Research, Mozilla, the PwC Center, Amazon AI, JP Morgan Chase, the Block Center, the Center for Machine Learning and Health, and the CMU Software Engineering Institute (SEI) via Department of Defense contract FA8702-15-D-0002, for their generous support of our research. We also thank Monica Agrawal, Ahmed Alaa, and Shan Chen for helpful discussions on an earlier version of this manuscript.

## Appendix A. Additional Details on Datasets

Table A1: The numbers of train, validation, and test QA examples for all textual medical knowledge QA, textual clinical note QA, and visual medical QA datasets used for evaluation.

QA Type	Dataset	Train	Validation	Test
Textual Medical Knowledge QA	MedQA (4 & 5 Options)	10178	1272	1273
	MedMCQA	146257	36565	4183
	PubMedQA	211269	500	500
	MMLU (Anatomy)	5	14	135
	MMLU (Clinical Knowledge)	5	29	265
	MMLU (College Biology)	5	16	144
	MMLU (College Medicine)	5	22	173
	MMLU (High School Biology)	5	32	310
	MMLU (Medical Genetics)	5	11	100
	MMLU (Nutrition)	5	33	306
	MMLU (Professional Medicine)	5	31	272
	MMLU (Virology)	5	18	166
Textual Clinical Note QA	MedNLI	11232	1395	1422
	EHRNoteQA	319	105	105
	i2b2 2008 Challenge (Asthma)	457	115	357
	i2b2 2008 Challenge (CAD)	441	111	335
	i2b2 2008 Challenge (Diabetes)	457	115	358
	i2b2 2008 Challenge (Obesity)	443	111	334
	CASI Sense Disambiguation	9978	3304	3304
	MIMIC-III Sense Disambiguation	10384	3458	3458
	VQA-RAD	820	205	272
	PathVQA	9806	3135	3391
Visual Medical QA	SLAKE	1943	422	415
	MMMU (Basic Medical Science)	5	5	25
	MMMU (Clinical Medicine)	5	5	25
	MMMU (Diag. & Lab Medicine)	5	5	25
	MMMU (Pharmacy)	5	5	25
	MMMU (Public Health)	5	5	25

For VQA-RAD (Lau et al., 2018), PathVQA (He et al., 2020), and SLAKE (Liu et al., 2021), we only show the number of *closed-ended* examples, since we focus on closed-ended QA. For the datasets that required additional splits from the official train-validation-test split (e.g., due to the lack of a public test set), we include all of the fixed random seeds.

## Appendix B. Additional Details on Model-Specific Prompt Selection

To define the prompt format search space discussed in Section 3.1, we construct a context-free grammar of plausible prompt formats following Sclar et al. (2024) (see Section 3.1 and Appendix A of the paper for reference). Using the Backus-Naur notation, we first define the basic fields  $H_q$  for the question header (e.g., “### Question:”),  $H_c$  for the answer choice header (e.g., “### Options:”), and  $H_a$  for the answer header (e.g., “### Answer:”) as

$$\begin{aligned}
 H_q(f_{\text{case}}, d_q, s_1) &::= f_{\text{case}}(d_q)s_1\langle\text{text}\rangle, \\
 H_c(f_{\text{case}}, d_c, s_1) &::= f_{\text{case}}(d_c)s_1, \\
 H_a(f_{\text{case}}, d_a, s_1) &::= f_{\text{case}}(d_a)s_1\langle\text{text}\rangle,
 \end{aligned}$$

where  $f_{\text{case}} \in \mathcal{F}_{\text{case}}$  denotes the casing function (e.g.,  $x \mapsto \#\#\# + x$ ,  $x \mapsto x.\text{upper}()$ ),  $d_q \in D_q$  denotes the question descriptor (e.g., “Question”),  $d_c \in D_c$  denotes the answer

choice descriptor (e.g., “**Options**”),  $d_a \in D_a$  denotes the answer descriptor (e.g., “**Answer**”),  $s_1 \in S_1$  denotes the header separator (e.g., ‘:’), and  $\langle \text{text} \rangle$  denotes a text placeholder. For formatting the list of answer choices, we also define the basic fields  $C$  for formatting each answer choice (e.g., “(A) **yes**”) and  $L$  for the concatenation of all answer choices as follows:

$$C(f_{\text{wrap}}, f_{\text{index}}, i) ::= f_{\text{wrap}}(f_{\text{index}}(i))\langle \text{text} \rangle,$$

$$L(f_{\text{wrap}}, f_{\text{index}}, n, s_2) ::= C(f_{\text{wrap}}, f_{\text{index}}, 0)s_2 \dots s_2 C(f_{\text{wrap}}, f_{\text{index}}, n-1),$$

where  $f_{\text{wrap}} \in \mathcal{F}_{\text{wrap}}$  denotes the wrapper function for the answer choice letter (e.g.,  $x \mapsto “(“ + x + “)”$ ),  $f_{\text{index}} \in \mathcal{F}_{\text{index}}$  denotes the numbering function that converts an integer index into a number format (e.g.,  $0 \rightarrow “A”$ ),  $i \in \mathbb{Z}^+$  denotes the index of a particular answer choice from the list,  $s_2 \in S_2$  denotes the answer choice separator,  $n$  denotes the number of answer choices, and  $\langle \text{text} \rangle$  denotes a text placeholder. The full prompt format  $P(f_{\text{case}}, f_{\text{wrap}}, f_{\text{index}}, d_q, d_c, d_a, s_1, s_2, n)$  is then constructed by concatenating all of the headers and the answer choices, while adding space  $t \in T$  (e.g., “\n”) in-between:

$$P ::= H_q t H_c t L t H_a, \quad (1)$$

where we exclude the arguments for simplicity. To define the prompt format search space, we instantiate the grammar with the descriptors, separators, spaces, and functions shown below.

### Descriptors:

$$D_q = \{“\text{Question}”, “\”\};$$

$$D_c = \{“\text{Options}”, “\text{Choices}”, “\”\};$$

$$D_a = \{“\text{Answer}”, “\text{The answer is}”\}.$$

### Separators:

$$S_1 = \{“:”, “:”, “::”, “:\n”, “=”, “=”, “==”, “=\n”, “-”, “--”, “---”, “\n”, “\n\n”\};$$

$$S_2 = \{“\n”, “\n”, “;”, “||”, “”, “;\n”, “;\n\n”, “, ”\}.$$

### Spaces:

$$T = \{“\n”, “\n”, “||”, “ ”\}.$$

### Casing, Wrapper, and Numbering Functions:

$$\mathcal{F}_{\text{case}} = \{x \mapsto x, x \mapsto x.\text{title}(), x \mapsto x.\text{upper}(), x \mapsto x.\text{lower}(), x \mapsto “\#\#\# ” + x, x \mapsto “**” + x + “**”\};$$

$$\mathcal{F}_{\text{wrap}} = \{x \mapsto “(“ + x + “)”, x \mapsto x + “.”, x \mapsto x + “)”, x \mapsto “[” + x + “]”, x \mapsto x + “ )”, x \mapsto “<” + x + “>”\};$$

$$\mathcal{F}_{\text{index}} = \{x \mapsto \text{chr}(\text{ord}("A") + x)\}.$$

To randomly sample a prompt format accepted by the grammar, we randomly sample each of these components and construct the full prompt format as in Eq. (1). Below, we show an example QA pair from the MedQA dataset, formatted according to the formats sampled from the prompt format space defined by the above context-free grammar.

**Example 1**

A key factor facilitating the application of nested case-control studies from the MACS was:

OPTIONS – A ) Data collection  
 B ) Establishment of a repository of biologic specimens  
 C ) Participant interest  
 D ) Administration of the questionnaire by staff

THE ANSWER IS – B ) Establishment of a repository of biologic specimens

**Example 2**

QUESTION – A key factor facilitating the application of nested case-control studies from the MACS was:

CHOICES – [A] Data collection; [B] Establishment of a repository of biologic specimens; [C] Participant interest; [D] Administration of the questionnaire by staff

ANSWER – [B] Establishment of a repository of biologic specimens

## Appendix C. Additional Details on Zero-/Few-shot Prompting

Here, we summarize the prompting details made available for the medical LLMs and VLMs used in our evaluation (Appendix C.1), and the default prompt formats used for each LLM (Appendix C.2) and VLM (Appendix C.3), which have been reproduced based on the former.

### C.1 Reproducibility of Prompting Details

In Table C1, we provide a summary of all of the prompting details available (in the context of closed-ended medical QA) for all medical LLMs and VLMs used in our evaluation. We share these details to demonstrate our best efforts with reproducing the original prompting setups considered for performing our evaluations. In particular, we focus on whether the following four components are explicitly made available, either in the original publications or the publicly released code repository: (i) system prompt; (ii) zero-/few-shot prompt format (used for closed-ended QA tasks); (iii) the choice of few-shot examples; and (iv) details on how the text generations are sampled (e.g., softmax temperature, top- $p$ , beam size, random seeds used for sampling). Below, we provide detailed clarifications for each model.

**MED42-v2 (Christophe et al., 2024b).** We follow the instructions provided in the model cards on HuggingFace, for the 70B-parameter<sup>3</sup> and 8B-parameter<sup>4</sup> models. We use the recommended system prompt and the LLAMA-3-based conversational prompt format. Meanwhile, in Table C1, we treat the prompt format as partially missing, as the exact format that was used to format each question (“user” query) and answer (“assistant” response) for evaluation on closed-ended multiple-choice questions is not provided. As Christophe et al.

3. [huggingface.co/m42-health/Llama3-Med42-70B](https://huggingface.co/m42-health/Llama3-Med42-70B)

4. [huggingface.co/m42-health/Llama3-Med42-8B](https://huggingface.co/m42-health/Llama3-Med42-8B)

Table C1: Summary of prompting details shared for each medical LLM and VLM in the original papers. For each column, a  $\checkmark$  indicates that the information was fully provided, and a  $\blacktriangle$  indicates that the information was partially provided (e.g., random sampling without information about the seeds). Otherwise, the information was either not provided or irrelevant (e.g., no few-shot example details due to lack of few-shot evaluations).

Model	System Prompt	Prompt Format	Few-Shot Examples	Sampling Details
MED42-v2	$\checkmark$	$\blacktriangle$		$\checkmark$
MED42-v1	$\checkmark$	$\checkmark$		$\checkmark$
OPENBIO-LLM	$\checkmark$	$\blacktriangle$		
CLINICAL-CAMEL		$\blacktriangle$		$\blacktriangle$
BIO-MISTRAL	$\checkmark$	$\checkmark$		$\blacktriangle$
MEDI-TRON	$\checkmark$	$\blacktriangle$	$\checkmark$	$\checkmark$
BIO-MEDGPT-LM				
LLAVA-MED	$\blacktriangle$	$\blacktriangle$		$\blacktriangle$
MED-FLAMINGO	$\checkmark$	$\blacktriangle$		

(2024a) include the prompt format used for MED42-v1, we use this format since both models are from the same authors. In the original evaluation, the model predictions are selected based on the log-likelihood of each answer choice, which differs from our evaluation setup. We include the default prompt format used for MED42-v2 in Appendix C.2.1.

**MED42-v1 (Christophe et al., 2024a).** We follow the instructions provided in the model card<sup>5</sup> on HuggingFace. We use the recommended system prompt and the custom conversational prompt format with special `<|system|>`, `<|prompter|>`, and `<|assistant|>` tokens. For the prompt format, we refer to what is provided in Appendix A.1 of Christophe et al. (2024a). In the original evaluation, the model predictions are selected based on the log-likelihood of each answer choice, which differs from our evaluation setup (Section 3). We include the default prompt format used for MED42-v2 in Appendix C.2.2.

**OPENBIO-LLM (Pal and Sankarasubbu, 2024).** We follow the instructions provided in the model cards on HuggingFace, for the 70B-parameter<sup>6</sup> and 8B-parameter<sup>7</sup> models. We use the recommended system prompt and the LLAMA-3-based conversational prompt format. In Table C1, we treat the prompt format as partially missing, as the exact format used to format each question (“user” query) and answer (“assistant” response) for closed-ended multiple-choice QA is not provided. At the time of writing, there are no additional details about the models that have been publicly released, beyond what is provided in the model cards. We include the default prompt format used for OPENBIO-LLM in Appendix C.2.3.

**CLINICAL-CAMEL (Toma et al., 2023).** We use the conversation format used in the official GitHub repository, which corresponds to that of LLAMA-2 (Touvron et al., 2023b). As the system prompts and few-shot examples used for the main evaluations in the paper are not provided, we use our own manually designed default system prompt and search over

5. [huggingface.co/m42-health/med42-70b](https://huggingface.co/m42-health/med42-70b)

6. [huggingface.co/aaditya/Llama3-OpenBioLLM-70B](https://huggingface.co/aaditya/Llama3-OpenBioLLM-70B)

7. [huggingface.co/aaditya/Llama3-OpenBioLLM-8B](https://huggingface.co/aaditya/Llama3-OpenBioLLM-8B)

different choices of few-shot examples. For sampling, the evaluation code<sup>8</sup> uses default temperature setting of 0.7 (albeit without the random seeds), which differs from our evaluation setup. We include the default prompt format used for CLINICAL-CAMEL in Appendix C.2.4.

**BIOISTRAL (Labrak et al., 2024).** We use the system prompt and zero-/few-shot prompt format provided in Appendix F of the paper. At the time of writing, the code repository is not publicly available, and the few-shot example details are not fully disclosed. In Section 4.3 of Labrak et al. (2024), the authors mention that the output vocabulary is constrained to be one of the answer choices in lettered format (e.g., one of [“A”,“B”,“C”,“D”]) to force the model to avoid generating irrelevant tokens in its output. However, it is unclear whether (i) the filtered token with the highest probability was treated as the model’s prediction or (ii) a token was randomly sampled based on the re-normalized token probabilities. We include the default prompt format used for BIOISTRAL in Appendix C.2.5.

**MEDI TRON (Chen et al., 2023).** We use the system prompts—tailored specifically to MedQA, MedMCQA, PubMedQA, and the MMLU datasets—provided in Table 2 of the paper. For the prompt formats, we use the ones provided in the official GitHub repository, as the prompt formats (those with special ‘<|im\_start|>’ and ‘<|im\_end|>’ tokens, following the ChatML format<sup>9</sup>) shown in the paper are only applicable to the fine-tuned models (see this discussion<sup>10</sup> from the official GitHub repository). In particular, we refer to the prompt formats provided in the code<sup>11</sup> code and used for evaluation<sup>12</sup> to determine the default prompt format for both the 70B- and 7B-parameter models. However, we were unable to reliably reproduce the zero-/few-shot prompting performance using this prompt format, and therefore perform a grid search over the prompt formats as well for model-specific prompt selection. In the evaluation code<sup>13</sup>, Chen et al. (2023) provide the random seeds used for sampling the few-shot examples; however, we also search over the set of few-shot examples to consider a larger number of few-shot example choices. For sampling, we use the same greedy decoding approach as considered in the paper (“Top Token Selection” in Section 4.3 of the paper). We include the default prompt format used for MEDI TRON in Appendix C.2.6.

**BIO MEDGPT-LM (Luo et al., 2023).** While BIO MEDGPT-LM was evaluated on medical knowledge QA tasks such as MedMCQA and PubMedQA, it was only evaluated in the SFT regime, and the prompt formats used for these datasets are not available to the best of our knowledge. Meanwhile, the official GitHub repository provides Jupyter notebook examples<sup>14</sup> with a conversation format used in the context of other QA tasks. We thus use this format by default but search over the prompt formats for model-specific prompt selection, since it is not specifically designed for closed-ended multiple-choice QA tasks. Moreover, as the system prompt provided is not semantically applicable to the QA tasks that we consider (e.g., “You are working as an excellent assistant in chemistry and molecule di-

8. [github.com/bowang-lab/clinical-camel/blob/14d960f/evaluation/get\\_model\\_answer.py#L54](https://github.com/bowang-lab/clinical-camel/blob/14d960f/evaluation/get_model_answer.py#L54)

9. [github.com/openai/openai-python/blob/release-v0.28.0/chatml.md](https://github.com/openai/openai-python/blob/release-v0.28.0/chatml.md)

10. [github.com/epfLLM/meditron/issues/13#issuecomment-1845955741](https://github.com/epfLLM/meditron/issues/13#issuecomment-1845955741)

11. [github.com/epfLLM/meditron/blob/a7c7/evaluation/benchmarks.py#L622](https://github.com/epfLLM/meditron/blob/a7c7/evaluation/benchmarks.py#L622)

12. [github.com/epfLLM/meditron/blob/a7c7/evaluation/inference.py#L188](https://github.com/epfLLM/meditron/blob/a7c7/evaluation/inference.py#L188)

13. [github.com/epfLLM/meditron/blob/a7c7/evaluation/inference.py#L188](https://github.com/epfLLM/meditron/blob/a7c7/evaluation/inference.py#L188)

14. [github.com/PharMolix/OpenBioMed/blob/main/examples/biomedgpt\\_inference.ipynb](https://github.com/PharMolix/OpenBioMed/blob/main/examples/biomedgpt_inference.ipynb)

scovery.’’, we use our own manually designed default system prompt. We include the default prompt format used for BIOMEDGPT-LM in Appendix C.2.7.

**LLAVA-MED (Li et al., 2023a).** For LLAVA-MED, we use the system prompt and conversational prompt format in the “simple\_conv\_med” template<sup>15</sup> from the official GitHub repository (for LLAVA-v0 (Liu et al., 2023), we use the “simple\_conv” template<sup>16</sup>) by default. For formatting the visual questions, we refer to this file<sup>17</sup> containing the raw visual QA results on VQA-RAD (“Please choose from the following two options: [yes, no]”). Meanwhile, we make these choices with the following caveats, to the best of our knowledge. First, the exact choice of system prompt and conversational prompt format used for evaluation are not discussed in the paper or the code repository, and we choose the one that has a system prompt specific to LLAVA-MED (“You are LLaVA-Med, a large language and vision assistant trained by a group of researchers at Microsoft . . .”) and follows the conversational format used for VICUNA-v0 (Chiang et al., 2023), which forms its LLM backbone. Second, details on how the answer choices should be formatted in the context of closed-ended QA tasks is only shown in the VQA-RAD results file. Given the uncertainty in such details, we also search over the prompt formats for model-specific prompt selection. We note that LLAVA-MED was not pretrained on multi-image inputs or evaluated in the few-shot setting, and therefore details on the choice of few-shot examples are irrelevant. For sampling, the evaluation code<sup>18</sup> uses a temperature setting of 0.7 (albeit without the random seeds), which differs from our evaluation setup. We include the default prompt formats used for LLAVA-MED and LLAVA-v0 in Appendices C.3.1–C.3.2.

**MED-FLAMINGO (Moor et al., 2023b).** We by default use the system prompt and prompt format provided in the demo code<sup>19</sup> from the official GitHub repository. However, we search over the prompt formats when performing model-specific prompt selection, as the example prompt in the demo does not show details for formatting answer choices in a closed-ended QA context. The choice of few-shot examples and sampling details used for the original evaluations on VQA-RAD and PathVQA are not available. We include the default prompt formats used for MED-FLAMINGO and OPEN-FLAMINGO in Appendices C.3.3–C.3.4.

## C.2 Default LLM Prompt Formats

Here, we share the *default* prompt formats for each LLM, with MMLU (Clinical Knowledge) (Hendrycks et al., 2021) as a running example. We denote the system prompt in **orange**, the few-shot examples in **green**, and the question in **pink**. For models without a specific system prompt and prompt format designed for closed-ended medical QA (Section C.1), we use a manually designed prompt format by default. This includes all general-domain LLMs. For example, the default 1-shot prompt for non-instruction-tuned models is as follows:

15. [github.com/microsoft/LLaVA-Med/blob/b9a9/llava/conversation.py#L243](https://github.com/microsoft/LLaVA-Med/blob/b9a9/llava/conversation.py#L243)

16. [github.com/microsoft/LLaVA-Med/blob/b9a9/llava/conversation.py#L257](https://github.com/microsoft/LLaVA-Med/blob/b9a9/llava/conversation.py#L257)

17. [github.com/microsoft/LLaVA-Med/blob/b9a9/llava/eval/eval\\_metrics/answer-file-llava-zeorshot.jsonl](https://github.com/microsoft/LLaVA-Med/blob/b9a9/llava/eval/eval_metrics/answer-file-llava-zeorshot.jsonl)

18. [github.com/microsoft/LLaVA-Med/blob/b9a9/llava/eval/model\\_vqa\\_med.py](https://github.com/microsoft/LLaVA-Med/blob/b9a9/llava/eval/model_vqa_med.py)

19. [github.com/snap-stanford/med-flamingo/blob/7bcb/scripts/demo.py](https://github.com/snap-stanford/med-flamingo/blob/7bcb/scripts/demo.py)

The following is a multiple-choice question about medical knowledge. Answer the question by choosing one of the options from A to D.

### Question: Glycolysis is the name given to the pathway involving the conversion of:

- (A) glycogen to glucose-1-phosphate.
- (B) glycogen or glucose to fructose.
- (C) glycogen or glucose to pyruvate or lactate.
- (D) glycogen or glucose to pyruvate or acetyl CoA.

### Answer: (C) glycogen or glucose to pyruvate or lactate.

### Question: What size of cannula would you use in a patient who needed a rapid blood transfusion (as of 2020 medical knowledge)?

- (A) 18 gauge.
- (B) 20 gauge.
- (C) 22 gauge.
- (D) 24 gauge.

### Answer:

For instruction-tuned models, which expect a specific *conversational* format, we apply the above format to each “user” query and “assistant” response and remove the ‘###’ and ‘Answer:’ tags. For example, the input prompt to LLAMA-3-70B-INSTRUCT is as follows:

```
<|begin_of_text|><|start_header_id|> system <|end_header_id|>
The following is a multiple-choice question about medical knowledge. Answer the question by choosing one of the options from A to D.<|eot_id|>
<|start_header_id|>user<|end_header_id|> Question: Glycolysis is the name given to the pathway involving the conversion of:
(A) glycogen to glucose-1-phosphate.
(B) glycogen or glucose to fructose.
(C) glycogen or glucose to pyruvate or lactate.
(D) glycogen or glucose to pyruvate or acetyl CoA.<|eot_id|>
<|start_header_id|>assistant<|end_header_id|>
(C) glycogen or glucose to pyruvate or lactate.<|eot_id|>
<|start_header_id|>user<|end_header_id|>
Question: What size of cannula would you use in a patient who needed a rapid blood transfusion (as of 2020 medical knowledge)?
(A) 18 gauge.
(B) 20 gauge.
(C) 22 gauge.
(D) 24 gauge.<|eot_id|>
<|start_header_id|>assistant<|end_header_id|>
```

In the following subsections, we show the system prompt and prompt formats used in the 1-shot setting for models that have a dedicated format. We exclude the model-specific special tokens (e.g., ‘[INST]’) for ease of presentation, and add ‘[User]’ and ‘[Model]’ to demarcate each question and answer for the instruction-tuned models.

C.2.1 MED42-v2 (CHRISTOPHE ET AL., 2024B)

You are a helpful, respectful and honest medical assistant. You are a second version of Med42 developed by the AI team at M42, UAE. Always answer as helpfully as possible, while being safe. Your answers should not include any harmful, unethical, racist, sexist, toxic, dangerous, or illegal content. Please ensure that your responses are socially unbiased and positive in nature. If a question does not make any sense, or is not factually coherent, explain why instead of answering something not correct. If you don't know the answer to a question, please don't share false information.

**[User]** Question: Glycolysis is the name given to the pathway involving the conversion of:

- (A) glycogen to glucose-1-phosphate.
- (B) glycogen or glucose to fructose.
- (C) glycogen or glucose to pyruvate or lactate.
- (D) glycogen or glucose to pyruvate or acetyl CoA.

**[Model]** (C) glycogen or glucose to pyruvate or lactate.

**[User]** Question: What size of cannula would you use in a patient who needed a rapid blood transfusion (as of 2020 medical knowledge)?

- (A) 18 gauge.
- (B) 20 gauge.
- (C) 22 gauge.
- (D) 24 gauge.

C.2.2 MED42-v1 (CHRISTOPHE ET AL., 2024A)

<|system|>: You are a helpful medical assistant created by M42 Health in the UAE.  
<|prompter|>: Question: Glycolysis is the name given to the pathway involving the conversion of:

- (A) glycogen to glucose-1-phosphate.
- (B) glycogen or glucose to fructose.
- (C) glycogen or glucose to pyruvate or lactate.
- (D) glycogen or glucose to pyruvate or acetyl CoA.

<|assistant|>: (C) glycogen or glucose to pyruvate or lactate.

<|prompter|>: Question: What size of cannula would you use in a patient who needed a rapid blood transfusion (as of 2020 medical knowledge)?

- (A) 18 gauge.
- (B) 20 gauge.
- (C) 22 gauge.
- (D) 24 gauge.

C.2.3 OPENBIOILLM (PAL AND SANKARASUBBU, 2024)

You are an expert and experienced from the healthcare and biomedical domain with extensive medical knowledge and practical experience. Your name is OpenBioILLM, and you were developed by Saama AI Labs. who's willing to help answer the user's query

with explanation. In your explanation, leverage your deep medical expertise such as relevant anatomical structures, physiological processes, diagnostic criteria, treatment guidelines, or other pertinent medical concepts. Use precise medical terminology while still aiming to make the explanation clear and accessible to a general audience.

**[User]** Question: Glycolysis is the name given to the pathway involving the conversion of:

- (A) glycogen to glucose-1-phosphate.
- (B) glycogen or glucose to fructose.
- (C) glycogen or glucose to pyruvate or lactate.
- (D) glycogen or glucose to pyruvate or acetyl CoA.

**[Model]** (C) glycogen or glucose to pyruvate or lactate.

**[User]** Question: What size of cannula would you use in a patient who needed a rapid blood transfusion (as of 2020 medical knowledge)?

- (A) 18 gauge.
- (B) 20 gauge.
- (C) 22 gauge.
- (D) 24 gauge.

#### C.2.4 CLINICAL-CAMEL (TOMA ET AL., 2023)

The following is a multiple-choice question about medical knowledge. Answer the question by choosing one of the options from A to D.

**[User]** Question: Glycolysis is the name given to the pathway involving the conversion of:

- (A) glycogen to glucose-1-phosphate.
- (B) glycogen or glucose to fructose.
- (C) glycogen or glucose to pyruvate or lactate.
- (D) glycogen or glucose to pyruvate or acetyl CoA.

**[Model]** (C) glycogen or glucose to pyruvate or lactate.

**[User]** Question: What size of cannula would you use in a patient who needed a rapid blood transfusion (as of 2020 medical knowledge)?

- (A) 18 gauge.
- (B) 20 gauge.
- (C) 22 gauge.
- (D) 24 gauge.

#### C.2.5 BIOMISTRAL (LABRAK ET AL., 2024)

The following are multiple choice questions (with answers) about medical knowledge.

\*\*Question:\*\* Glycolysis is the name given to the pathway involving the conversion of:

- (A) glycogen to glucose-1-phosphate.
- (B) glycogen or glucose to fructose.
- (C) glycogen or glucose to pyruvate or lactate.

(D) glycogen or glucose to pyruvate or acetyl CoA.

\*\*Answer:\*\* (C

\*\*Question:\*\* What size of cannula would you use in a patient who needed a rapid blood transfusion (as of 2020 medical knowledge)?

(A) 18 gauge.

(B) 20 gauge.

(C) 22 gauge.

(D) 24 gauge.

\*\*Answer:\*\* (

#### C.2.6 MEDI TRON (CHEN ET AL., 2023)

You are a medical doctor answering real-world medical entrance exam questions. Based on your understanding of basic and clinical science, medical knowledge, and mechanisms underlying health, disease, patient care, and modes of therapy, answer the following multiple-choice question. Select one correct answer from A to D. Base your answer on the current and standard practices referenced in medical guidelines.

Question: Glycolysis is the name given to the pathway involving the conversion of:

Options:

A. glycogen to glucose-1-phosphate.

B. glycogen or glucose to fructose.

C. glycogen or glucose to pyruvate or lactate.

D. glycogen or glucose to pyruvate or acetyl CoA.

The answer is: C

Question: What size of cannula would you use in a patient who needed a rapid blood transfusion (as of 2020 medical knowledge)?

Options:

A. 18 gauge.

B. 20 gauge.

C. 22 gauge.

D. 24 gauge.

The answer is:

#### C.2.7 BIOMEDGPT-LM (LUO ET AL., 2023)

The following is a multiple-choice question about medical knowledge. Answer the question by choosing one of the options from A to D.

### Human: Glycolysis is the name given to the pathway involving the conversion of:

(A) glycogen to glucose-1-phosphate.

(B) glycogen or glucose to fructose.

(C) glycogen or glucose to pyruvate or lactate.

(D) glycogen or glucose to pyruvate or acetyl CoA.

### Assistant: (C) glycogen or glucose to pyruvate or lactate.

### Human: What size of cannula would you use in a patient who needed a rapid blood transfusion (as of 2020 medical knowledge)?

- (A) 18 gauge.
- (B) 20 gauge.
- (C) 22 gauge.
- (D) 24 gauge.

### Assistant:

### C.3 Default VLM Prompt Formats

Here, we share the *default* prompt formats that we use for each VLM, using VQA-RAD (Lau et al., 2018) as a running example. We denote the system prompt in **orange**, the few-shot examples in **green**, and the question **pink**. We show the format in the 1-shot setting.

#### C.3.1 LLAVA-MED (LI ET AL., 2023A)

You are LLAVA-Med, a large language and vision assistant trained by a group of researchers at Microsoft, based on the general domain LLAVA architecture. You are able to understand the visual content that the user provides, and assist the user with a variety of medical and clinical tasks using natural language.

Follow the instructions carefully and explain your answers in detail.

### Human: Does this patient have multiple lesions in their chest? Please choose from the following options: [yes, no]. <image>

### Assistant: no

### Human: Is there evidence of an aortic aneurysm? Please choose from the following options: [yes, no]. <image>

### Assistant:

#### C.3.2 LLAVA-v0 (LIU ET AL., 2023)

A chat between a curious human and an artificial intelligence assistant. The assistant gives helpful, detailed, and polite answers to the human's questions.

### Human: Does this patient have multiple lesions in their chest? Please choose from the following options: [yes, no]. <image>

### Assistant: no

### Human: Is there evidence of an aortic aneurysm? Please choose from the following options: [yes, no]. <image>

### Assistant:

#### C.3.3 MED-FLAMINGO (MOOR ET AL., 2023B)

You are a helpful medical assistant. You are being provided with images, a question about the image and an answer. Follow the examples and answer the last question.

<image> Does this patient have multiple lesions in their chest?

- (A) yes
- (B) no

Answer: (B) no <|endofchunk|>

<image> Is there evidence of an aortic aneurysm?

(A) yes  
(B) no

Answer:

#### C.3.4 OPEN-FLAMINGO (AWADALLA ET AL., 2023)

The following is a multiple-choice visual question requiring medical knowledge. Answer the question by choosing one of the provided answer options.

<image> Does this patient have multiple lesions in their chest?

(A) yes  
(B) no

Answer: (B) no <|endofchunk|> <image> Is there evidence of an aortic aneurysm?

(A) yes  
(B) no

Answer:

## Appendix D. Zero-/Few-Shot Prompting Evaluation Results with Constrained Decoding

Table D1: The zero-shot and 3-shot win/tie/loss rates (%) of all medical LLMs on textual medical knowledge QA, after independently optimizing the prompt for each model. For each medical model, we boldface the win rate if it wins more than it loses to its general-domain base model, and vice versa. Here, we show the results when model predictions are generated via constrained decoding. The results for greedy decoding are shown in Table 3.

Model	Zero-Shot			3-Shot		
	Win	Tie	Loss	Win	Tie	Loss
OPENBIO-LLM-70B	7.7	76.9	<b>15.4</b>	23.1	53.8	23.1
MEDI-TRON-70B	<b>30.8</b>	46.2	23.1	15.4	69.2	15.4
CLINICAL-CAMEL-70B	<b>18.2</b>	72.7	9.1	9.1	72.7	<b>18.2</b>
OPENBIO-LLM-8B	0	53.8	<b>46.2</b>	7.7	69.2	<b>23.1</b>
MEDI-TRON-7B	<b>23.1</b>	76.9	0	<b>7.7</b>	92.3	0
BIO-MISTRAL-7B	<b>30.8</b>	69.2	0	<b>7.7</b>	92.3	0
BIO-MEDGPT-LM-7B	7.7	84.6	7.7	<b>7.7</b>	69.2	<b>23.1</b>
<b>Aggregate</b>	<b>16.9</b>	68.5	14.6	11.2	74.2	<b>14.6</b>

Here, we provide the constrained decoding results for the zero-/few-shot prompting evaluations described in Section 3.1 (see ‘‘Models’’ in Section 3 for a description on constrained decoding). In Appendices D.1–D.3, corresponding to Sections 4.1.1–4.1.3, we show the results on the textual medical knowledge QA, textual clinical note QA, and visual medical QA datasets, when model-specific prompt selection is performed for each model independently. In Appendix D.4, corresponding to Section 4.2.3, we show the aggregate results on how the win, tie, and loss rates (%) of the medical models are affected by the inclusion (or lack thereof) of model-specific prompt selection and statistical testing.

### D.1 Evaluation of Medical LLMs on Textual Medical Knowledge QA (Section 4.1.1)

In Figures D1(a) and (b), we show the absolute and relative exact-match accuracies achieved by the medical and general-domain LLMs on the textual medical knowledge QA datasets, from zero-shot and 3-shot prompting, respectively. In Table D1, we also show the win, tie, and loss rates (%) of the medical LLMs, where win rate refers to the proportion of QA datasets where a medical model shows a statistically significant improvement over its base model. We exclude the results for CLINICAL-CAMEL-70B on both versions of MedQA, and the MED42 models on all textual medical knowledge QA datasets, as they have already been trained on these datasets via medical DAPT (Table 2).

Overall, we observe that our findings discussed in Section 4.1.1 also hold in the constrained decoding setting. In particular, we observe that

1. medical and general-domain LLMs generally achieve higher accuracy across all datasets, going from the zero-shot to 3-shot setting;
2. more recent general-domain models (e.g., LLAMA-3-8B) tend to show stronger performance even without any medical adaptation via DAPT; and
3. the majority of medical LLMs show limited improvement over their base models, reaching a tie in most cases (aggregate zero-shot/3-shot tie rates of 68.5%/74.2%).

These results suggest that even when we constrain the outputs of each model to always produce a valid answer choice (which is not guaranteed with greedy decoding, especially in the zero-shot setting), the performance benefits from medical DAPT on textual medical knowledge QA datasets are overall limited in the zero-/few-shot prompting regime.

### D.2 Evaluation of Medical LLMs on Textual Clinical Note QA (Section 4.1.2)

In Figures D2(a) and (b), we show the absolute and relative exact-match accuracies achieved by the medical and general-domain LLMs on the textual clinical note QA datasets, from zero-shot and 3-shot prompting, respectively. In Figures D3(a) and (b), we show the absolute and relative *macro* exact-match accuracies and F1 scores—averaged over clinical acronyms—on the CASI and MIMIC-III sense disambiguation datasets, from zero-shot and 3-shot prompting, respectively. In Table D2, we also show the win, tie, and loss rates (%) of the medical LLMs, where win rate refers to the proportion of QA datasets where a medical model shows a statistically significant improvement over its base model. As discussed in Section 3.1, we exclude the EHRNoteQA and i2b2 datasets from few-shot prompting evaluations, as most of the clinical notes already occupy the full context window for most models even in the zero-shot setting. Additionally, we exclude the zero-shot results on these datasets for MEDI TRON-7B (and its base model LLAMA-2-7B), as its context window size of 2k tokens is insufficient even in the zero-shot setting.

Overall, we observe that our findings discussed in Section 4.1.2 also hold in the constrained decoding setting. In particular, we observe that

1. the extent of performance improvement achieved by medical LLMs varies significantly across different model pairs and datasets;

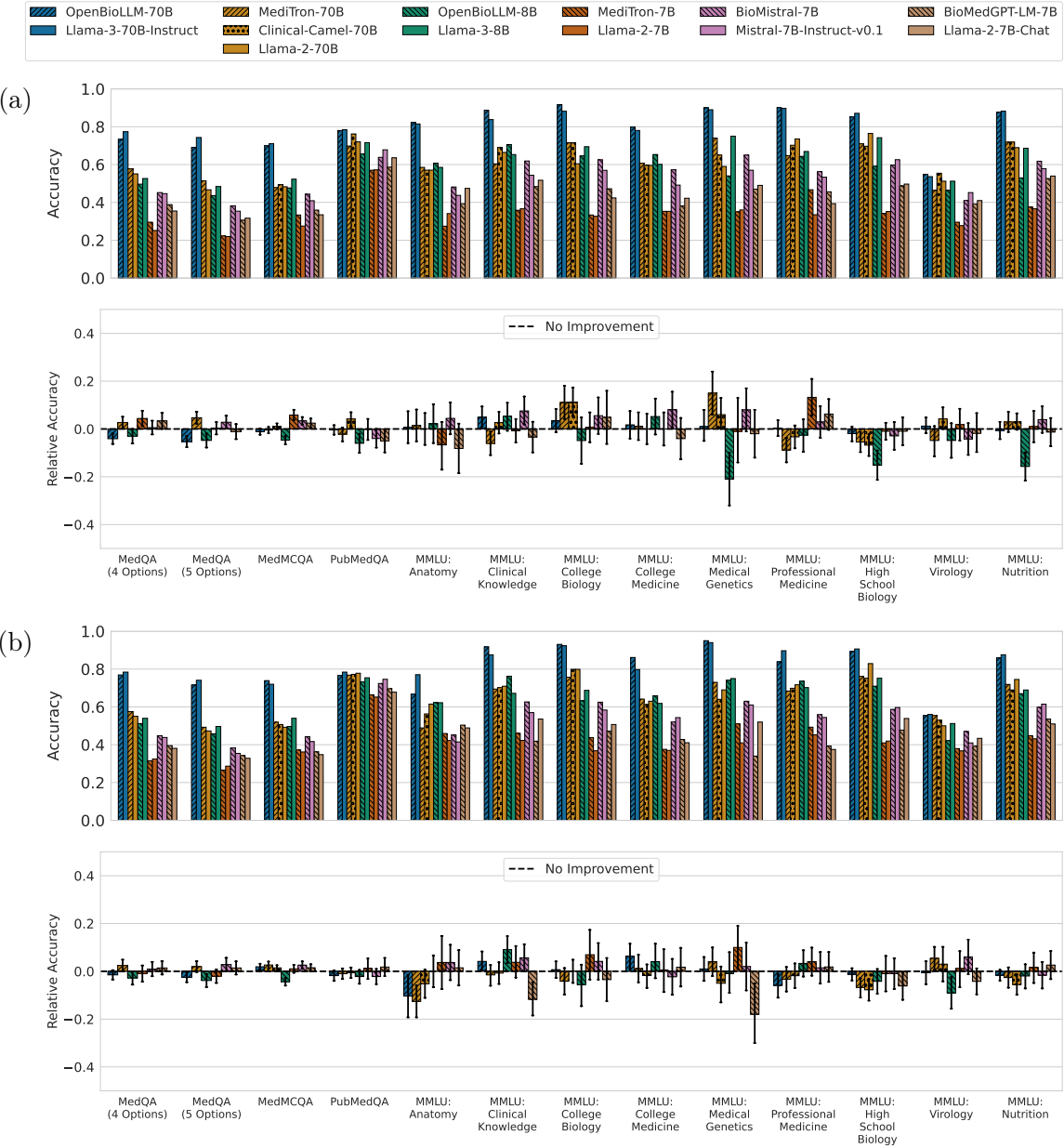


Figure D1: After independently selecting the best prompt format and examples for each model, medical LLMs (textured bars) fail to consistently improve over their base models (solid bars) on textual medical knowledge QA tasks, in both (a) zero-shot and (b) 3-shot settings. In each panel, the top row shows the absolute exact-match accuracies on the test set, and the bottom row shows the relative exact-match accuracies along with 95% confidence intervals derived via bootstrapping on the test set (Section 3). Here, model predictions are generated via constrained decoding. Greedy decoding results are shown in Figure 4.

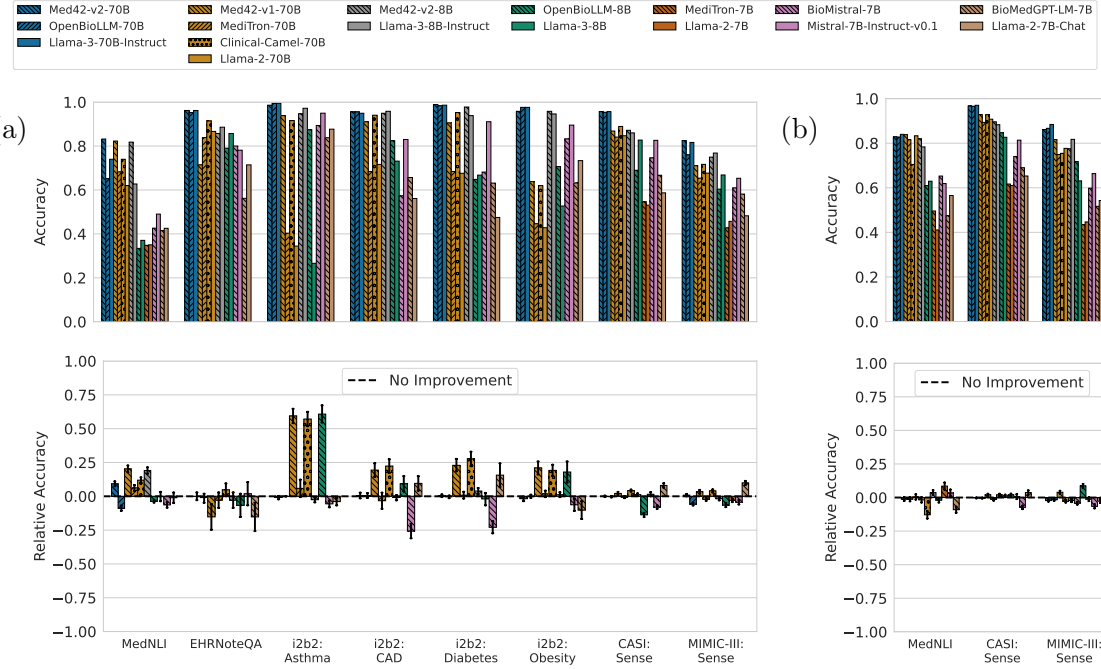


Figure D2: After independently selecting the best prompt format and examples for each model, medical LLMs (textured bars) fail to consistently improve over their base models (solid bars) on textual clinical note QA tasks, in both (a) zero-shot and (b) 3-shot settings. In the 3-shot setting, we exclude the results on the EHRNoteQA and i2b2 datasets given the context window limitations (Section 3.1). In each panel, the top row shows the absolute exact-match accuracies on the test set, and the bottom row shows the relative exact-match accuracies along with 95% confidence intervals derived via bootstrapping on the test set (Section 3). Here, model predictions are generated via constrained decoding. Greedy decoding results are shown in Figure 5.

2. the results vary the most on the i2b2 datasets (which involve full-length, minimally preprocessed clinical notes), with MED42-v1-70B and CLINICAL-CAMEL-70B showing the largest improvements as in the greedy decoding case;
3. only two medical LLMs—MED42-v1-70B and MED42-v2-8B—consistently show improvements in both zero-shot and 3-shot settings; and
4. medical LLMs and general-domain LLMs are virtually indistinguishable in terms of the aggregate win/tie/loss rates.

These results suggest that even when we constrain the outputs of each model to always produce a valid answer choice (which is not guaranteed with greedy decoding, especially in the zero-shot setting), the performance benefits from medical DAPT on textual clinical note QA datasets are overall limited in the zero-/few-shot prompting regime.

### D.3 Evaluation of Medical VLMs on Visual Medical QA (Section 4.1.3)

In Figures D4(a) and (b), we show the absolute and relative exact-match accuracies achieved by the medical and general-domain VLMs on the visual medical QA datasets, from zero-shot

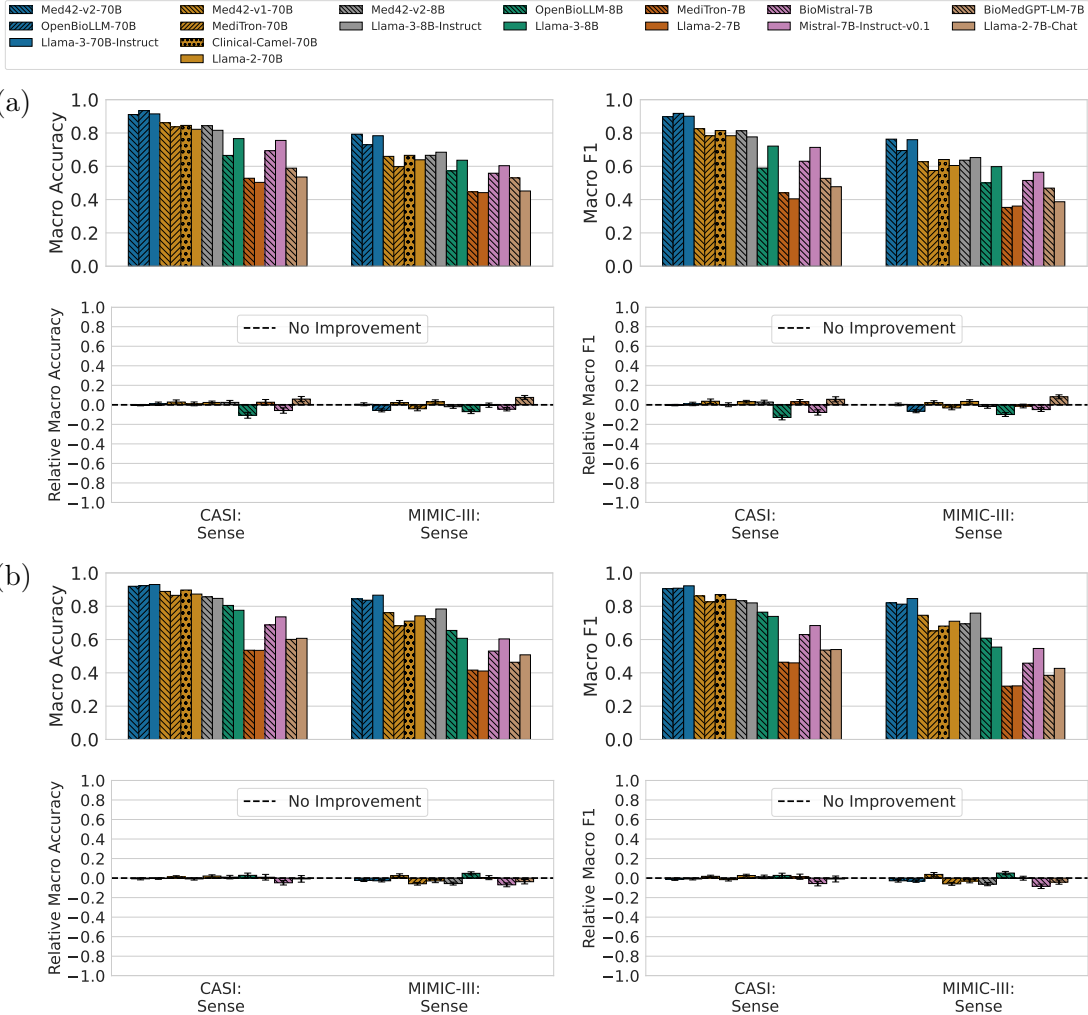


Figure D3: Even after accounting for the imbalance in the distribution of clinical acronyms in the CASI and MIMIC-III datasets, medical LLMs (textured bars) fail to consistently improve over their base models (solid bars), in both (a) zero-shot and (b) 3-shot settings. We show the results when the prompts are optimized for each model independently. In each panel, the top row shows the absolute macro exact-match accuracies and F1 scores—averaged over clinical acronyms—on the test set, and the bottom row shows the relative macro exact-match accuracies and F1 scores along with 95% confidence intervals derived via bootstrapping on the test set (Section 3). Here, model predictions are generated via constrained decoding. Greedy decoding results are shown in Figure 6.

and 3-shot prompting, respectively. Table D3 shows the win, tie, and loss rates (%) of the medical VLMs, where win rate refers to the proportion of visual medical QA datasets where a medical model shows a statistically significant improvement over its base model.

Overall, we observe that our findings discussed in Section 4.1.3 also hold in the constrained decoding setting. In particular, we observe that

Table D2: The zero-shot and 3-shot win, tie, and loss rates (%) of all medical LLMs on textual clinical note QA, after independently optimizing the prompt for each model. For each medical model, we boldface the win rate if it wins more than it loses to its general-domain base model, and vice versa. Here, we show the results when model predictions are generated via constrained decoding. The results for greedy decoding are shown in Table 4.

Model	Zero-Shot			3-Shot		
	Win	Tie	Loss	Win	Tie	Loss
MED42-v2-70B	12.5	75.0	12.5	0	66.7	<b>33.3</b>
OPENBIO-LLM-70B	0	75.0	<b>25.0</b>	0	33.3	<b>66.7</b>
MED42-v1-70B	<b>87.5</b>	0	0	<b>66.7</b>	33.3	0
MEDITRON-70B	12.5	75.0	12.5	0	33.3	<b>66.7</b>
CLINICAL-CAMEL-70B	<b>87.5</b>	12.5	0	33.3	0	<b>66.7</b>
MED42-v2-8B	<b>37.5</b>	37.5	25.0	<b>66.7</b>	0	33.3
OPENBIO-LLM-8B	37.5	25.0	37.5	<b>66.7</b>	0	33.3
MEDITRON-7B	0	66.7	<b>33.3</b>	<b>33.3</b>	66.7	0
BIO-MISTRAL-7B	0	12.5	<b>87.5</b>	33.3	0	<b>66.7</b>
BIO-MEDGPT-LM-7B	<b>50.0</b>	12.5	37.5	33.3	0	<b>66.7</b>
<b>Aggregate</b>	<b>34.7</b>	37.3	28.0	33.3	23.3	<b>43.3</b>

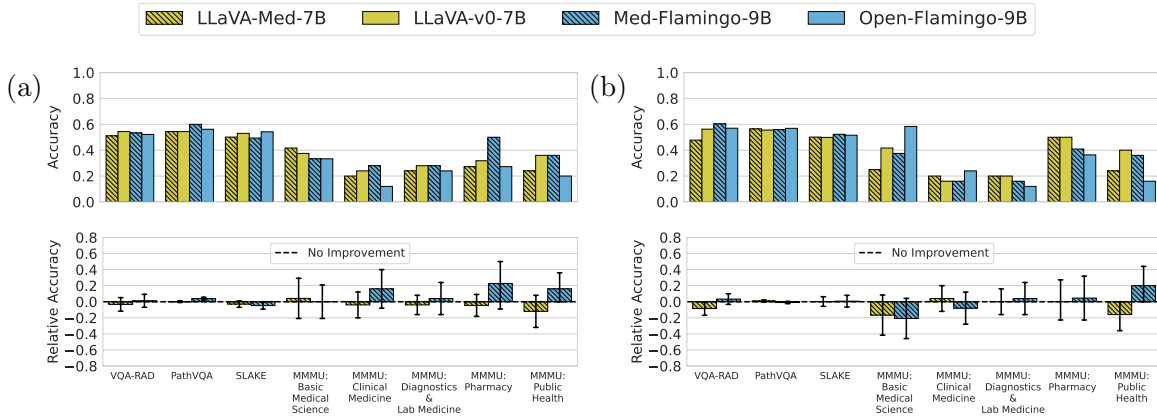


Figure D4: After independently selecting the best prompt format and examples for each model, medical VLMs (textured bars) fail to consistently improve over their base models (solid bars) on visual medical QA tasks, in both (a) zero-shot and (b) 3-shot settings. In each panel, the top row shows the absolute exact-match accuracies on the test set, and the bottom row shows the relative exact-match accuracies along with 95% confidence intervals derived via bootstrapping on the test set (Section 3). Here, model predictions are generated via constrained decoding. Greedy decoding results are shown in Figure 7.

1. the absolute accuracies of the medical and general-domain models are generally similar on VQA-RAD, PathVQA, and SLAKE;
2. the absolute accuracies do not consistently exhibit an increasing trend going from the zero-shot setting to the 3-shot setting; and

Table D3: The zero-shot and 3-shot win, tie, and loss rates (%) of all medical VLMs on visual medical QA, after independently optimizing the prompt for each model. For each medical model, we boldface the win rate if it wins more than it loses to its general-domain base model, and vice versa. Here, we show the results when model predictions are generated via constrained decoding. The results for greedy decoding are shown in Table 5.

Model	Zero-Shot			3-Shot		
	Win	Tie	Loss	Win	Tie	Loss
LLAVA-MED-7B	0	100.0	0	0	87.5	<b>12.5</b>
MED-FLAMINGO-9B	12.5	75.0	12.5	0	100.0	0
<b>Aggregate</b>	6.3	87.5	<b>6.3</b>	0	93.8	<b>6.3</b>

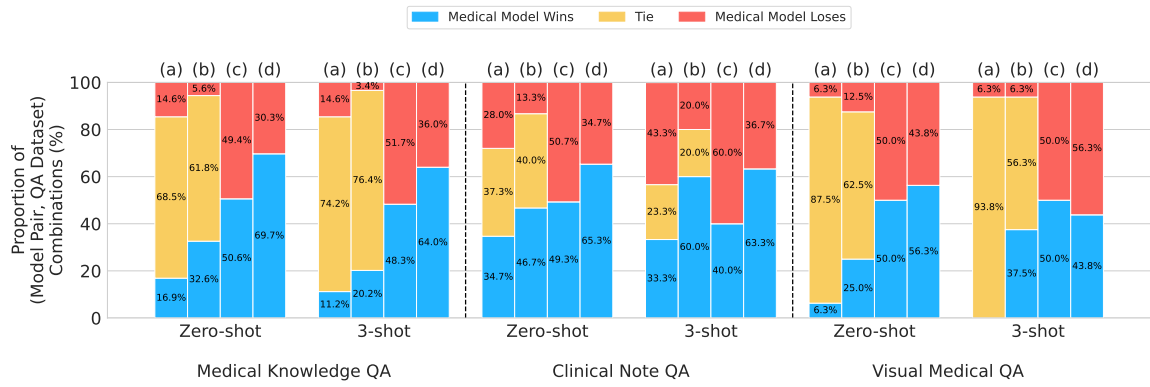


Figure D5: Optimizing the prompt for only the medical model and comparing models without accounting for statistical uncertainty can overestimate the performance improvements from medical DAPT. We show the win/tie/loss rates (%) of the medical models across all (model pair, QA dataset) combinations, when (a) optimizing the prompt for each model, with statistical testing; (b) optimizing the prompt only for the medical model, with statistical testing; (c) optimizing the prompt for each model, without statistical testing; and (d) optimizing the prompt only for the medical model, without statistical testing. Here, we show the results for constrained decoding. Greedy decoding results are shown in Figure 10.

3. the medical and general-domain VLMs are virtually indistinguishable in terms of the win/tie/loss rates (%) in both zero-shot and 3-shot settings.

These results suggest that even when we constrain the outputs of each model to always produce a valid answer choice (which is not guaranteed with greedy decoding, especially in the zero-shot setting), the performance benefits from medical DAPT on visual medical QA datasets are overall limited in the zero-/few-shot prompting regime.

#### D.4 Ignoring Prompt Sensitivity and Statistical Uncertainty Can Overestimate the Performance Benefits from Medical DAPT (Section 4.2.3)

In Figure D5, we show how the aggregate win/tie/loss rates (%) of the medical models, computed over all (model pair, QA dataset) combinations, change as we vary the prompting

setups as in Section 4.2.3. As with greedy decoding, we find that for both LLMs and VLMs, the performance improvements from medical DAPT can be substantially overestimated when (i) the prompt is only tailored to the medical model; and (ii) the models are compared only based on their absolute accuracies. For example, we observe that the zero-shot win rate substantially increases from 16.9% to 68.0% on textual medical knowledge QA, 32.5% to 61.6% on textual clinical note QA, and 6.3% to 56.3% on visual QA, when only performing prompt selection for the medical model and comparing based on raw absolute accuracy. Thus, even when we constrain the outputs of each model always produce a valid answer choice (which is not guaranteed with greedy decoding, especially in the zero-shot setting), it is essential to account for LLM/VLM sensitivity to the prompting details and statistical uncertainty, in order to draw reliable conclusions about the effectiveness of medical DAPT.

## Appendix E. Additional Details on Supervised Fine-Tuning (SFT)

### E.1 LoRA Fine-Tuning Details for LLMs

For all fine-tuning runs, we fix the  $\alpha$  hyperparameter in LoRA to 16 and search over the ranks  $r = [16, 32, 64]$  and the learning rates  $\eta = [10^{-5}, 2 \times 10^{-5}, 5 \times 10^{-5}, 10^{-4}, 2 \times 10^{-4}]$ , resulting in 15 trials per model and dataset. For each run, we train the model for a maximum of 10 epochs and apply early stopping regularization with a patience of 1 epoch. We track the validation cross-entropy loss on the output tokens after every epoch, and save the checkpoint that achieved the lowest validation loss during each fine-tuning run. We then select the model that achieved the lowest validation loss across all trials to use for final evaluation on the test set. Given the high variability in the remaining training details (e.g., per-device batch size  $B$ , the number of NVIDIA A6000 GPUs used for each run, the distributed training setup (DeepSpeed ZeRO Stage), use of QLoRA instead of LoRA) across different models and datasets, we detail them throughout Tables E1–E12, organized by dataset.

### E.2 LoRA Fine-Tuning Details for LLAVA-MED-7B and LLAVA-v0-7B

For all fine-tuning runs, we fix the  $\alpha$  hyperparameter in LoRA to 16 and search over the ranks  $r = [16, 32, 64]$ , the learning rates  $\eta = [10^{-5}, 2 \times 10^{-5}, 5 \times 10^{-5}]$ , and LoRA dropout  $p = [0, 0.1]$ , resulting in 18 trials per model and dataset. We fix the per-device batch size  $B$  to 32. For each run, we train the model for a maximum of 10 epochs and apply early stopping regularization with a patience of 1. We track the validation cross-entropy loss on the output tokens after every epoch, and save the checkpoint that achieved the lowest validation loss during each fine-tuning run. We then select the model with the lowest validation loss across all trials for final evaluation on the test set. We train all models using Stage 2 of DeepSpeed ZeRO (Rajbhandari et al., 2020), using 2 NVIDIA A6000 GPUs per trial.

### E.3 Fine-Tuning Details for MED-FLAMINGO-9B and OPEN-FLAMINGO-9B

For all fine-tuning runs, we search over the learning rates  $\eta = [10^{-5}, 2 \times 10^{-5}, 5 \times 10^{-5}]$  and the weight decay coefficients  $\lambda = [0, 0.05, 0.1]$ , resulting in 9 trials per model and dataset. We fix the per-device batch size  $B$  to 16. For each run, we train the model for a maximum of 10 epochs and apply early stopping regularization with a patience of 1. We track the validation cross-entropy loss on the output tokens after every epoch, and save the checkpoint that

achieved the lowest validation loss during each fine-tuning run. We then select the model with the lowest validation loss across all trials for final evaluation on the test set. We train all models using PyTorch FSDP (Zhao et al., 2023), using 6 NVIDIA A6000 GPUs per trial.

Table E1: MedQA (4 Opt.) SFT configs.

Model	$B$	# GPUs	ZeRO
OPENBIO-LLM-70B	8	8	3
LLAMA-3-70B-INSTRUCT	8	8	3
MEDI-TRON-70B	8	8	3
LLAMA-2-70B	8	8	3
OPENBIO-LLM-8B	16	2	2
LLAMA-3-8B	16	2	2
MEDI-TRON-7B	32	2	2
LLAMA-2-7B	32	2	2
BIO-MISTRAL-7B	32	2	2
MISTRAL-7B-INSTRUCT-v0.1	32	2	2
BIO-MEDGPT-LM-7B	32	2	2
LLAMA-2-7B-CHAT	32	2	2

Table E2: MedQA (5 Opt.) SFT configs.

Model	$B$	# GPUs	ZeRO
OPENBIO-LLM-70B	8	8	3
LLAMA-3-70B-INSTRUCT	8	8	3
MEDI-TRON-70B	8	8	3
LLAMA-2-70B	8	8	3
OPENBIO-LLM-8B	8	2	2
LLAMA-3-8B	8	2	2
MEDI-TRON-7B	32	2	2
LLAMA-2-7B	32	2	2
BIO-MISTRAL-7B	32	2	2
MISTRAL-7B-INSTRUCT-v0.1	32	2	2
BIO-MEDGPT-LM-7B	32	2	2
LLAMA-2-7B-CHAT	32	2	2

Table E3: MedMCQA SFT configs.

Model	$B$	# GPUs	ZeRO
OPENBIO-LLM-70B	2	8	3
LLAMA-3-70B-INSTRUCT	2	8	3
MEDI-TRON-70B	2	8	3
CLINICAL-CAMEL-70B	2	8	3
LLAMA-2-70B	2	8	3
OPENBIO-LLM-8B	16	4	2
LLAMA-3-8B	16	4	2
MEDI-TRON-7B	32	4	2
LLAMA-2-7B	32	4	2
BIO-MISTRAL-7B	32	4	2
MISTRAL-7B-INSTRUCT-v0.1	32	4	2
BIO-MEDGPT-LM-7B	32	4	2
LLAMA-2-7B-CHAT	32	4	2

Table E4: PubMedQA SFT configs.

Model	$B$	# GPUs	ZeRO
OPENBIO-LLM-70B (QLoRA)	2	8	2
LLAMA-3-70B-INSTRUCT (QLoRA)	2	8	2
MEDI-TRON-70B (QLoRA)	2	8	2
CLINICAL-CAMEL-70B (QLoRA)	2	8	2
LLAMA-2-70B (QLoRA)	2	8	2
OPENBIO-LLM-8B	8	4	2
LLAMA-3-8B	8	4	2
MEDI-TRON-7B	32	4	2
LLAMA-2-7B	32	4	2
BIO-MISTRAL-7B	32	4	2
MISTRAL-7B-INSTRUCT-v0.1	32	4	2
BIO-MEDGPT-LM-7B	32	4	2
LLAMA-2-7B-CHAT	32	4	2

Table E5: MedNLI SFT configs.

Model	$B$	# GPUs	ZeRO
MED42-v2-70B	8	8	3
OPENBIO-LLM-70B	8	8	3
LLAMA-3-70B-INSTRUCT	8	8	3
MEDI-TRON-70B	8	8	3
CLINICAL-CAMEL-70B	8	8	3
MED42-v1-70B	8	8	3
LLAMA-2-70B	8	8	3
MED42-v2-8B	16	2	2
LLAMA-3-8B-INSTRUCT	16	2	2
OPENBIO-LLM-8B	16	2	2
LLAMA-3-8B	16	2	2
MEDI-TRON-7B	32	2	2
LLAMA-2-7B	32	2	2
BIO-MISTRAL-7B	32	2	2
MISTRAL-7B-INSTRUCT-v0.1	32	2	2
BIO-MEDGPT-LM-7B	32	2	2
LLAMA-2-7B-CHAT	32	2	2

Table E6: CASI SFT configs.

Model	$B$	# GPUs	ZeRO
MED42-v2-70B	8	8	3
OPENBIO-LLM-70B	8	8	3
LLAMA-3-70B-INSTRUCT	8	8	3
MEDI-TRON-70B	8	8	3
CLINICAL-CAMEL-70B	8	8	3
MED42-v1-70B	8	8	3
LLAMA-2-70B	8	8	3
MED42-v2-8B	8	2	2
LLAMA-3-8B-INSTRUCT	8	2	2
OPENBIO-LLM-8B	8	2	2
LLAMA-3-8B	8	2	2
MEDI-TRON-7B	16	2	2
LLAMA-2-7B	16	2	2
BIO-MISTRAL-7B	16	2	2
MISTRAL-7B-INSTRUCT-v0.1	16	2	2
BIO-MEDGPT-LM-7B	16	2	2
LLAMA-2-7B-CHAT	16	2	2

Table E7: MIMIC-III SFT configs.

Model	$B$	# GPUs	ZeRO
MED42-v2-70B	8	8	3
OPENBIO-LLM-70B	8	8	3
LLAMA-3-70B-INSTRUCT	8	8	3
MEDI-TRON-70B	8	8	3
CLINICAL-CAMEL-70B	8	8	3
MED42-v1-70B	8	8	3
LLAMA-2-70B	8	8	3
MED42-v2-8B	8	2	2
LLAMA-3-8B-INSTRUCT	8	2	2
OPENBIO-LLM-8B	8	2	2
LLAMA-3-8B	8	2	2
MEDI-TRON-7B	32	2	2
LLAMA-2-7B	32	2	2
BIO-MISTRAL-7B	32	2	2
MISTRAL-7B-INSTRUCT-v0.1	32	2	2
BIO-MEDGPT-LM-7B	32	2	2
LLAMA-2-7B-CHAT	32	2	2

Table E9: i2b2 (Asthma) SFT configs.

Model	$B$	# GPUs	ZeRO
MED42-v2-70B	2	8	3
OPENBIO-LLM-70B	2	8	3
LLAMA-3-70B-INSTRUCT	2	8	3
MEDI-TRON-70B	2	8	3
CLINICAL-CAMEL-70B	2	8	3
MED42-v1-70B	2	8	3
LLAMA-2-70B	2	8	3
MED42-v2-8B	2	2	2
LLAMA-3-8B-INSTRUCT	2	2	2
OPENBIO-LLM-8B	2	2	2
LLAMA-3-8B	2	2	2
BIO-MISTRAL-7B	4	2	2
MISTRAL-7B-INSTRUCT-v0.1	4	2	2
BIO-MEDGPT-LM-7B	4	2	2
LLAMA-2-7B-CHAT	4	2	2

Table E11: i2b2 (Diabetes) SFT configs.

Model	$B$	# GPUs	ZeRO
MED42-v2-70B (QLoRA)	1	8	3
OPENBIO-LLM-70B (QLoRA)	1	8	3
LLAMA-3-70B-INSTRUCT (QLoRA)	1	8	3
MEDI-TRON-70B (QLoRA)	1	8	3
CLINICAL-CAMEL-70B (QLoRA)	1	8	3
MED42-v1-70B (QLoRA)	1	8	3
LLAMA-2-70B (QLoRA)	1	8	3
MED42-v2-8B	2	2	2
LLAMA-3-8B-INSTRUCT	2	2	2
OPENBIO-LLM-8B	2	2	2
LLAMA-3-8B	2	2	2
BIO-MISTRAL-7B	4	2	2
MISTRAL-7B-INSTRUCT-v0.1	4	2	2
BIO-MEDGPT-LM-7B	4	2	2
LLAMA-2-7B-CHAT	4	2	2

Table E8: EHRNoteQA SFT configs.

Model	$B$	# GPUs	ZeRO
MED42-v2-70B	4	8	3
OPENBIO-LLM-70B	4	8	3
LLAMA-3-70B-INSTRUCT	4	8	3
MEDI-TRON-70B	4	8	3
CLINICAL-CAMEL-70B	4	8	3
MED42-v1-70B	4	8	3
LLAMA-2-70B	4	8	3
MED42-v2-8B	4	2	2
LLAMA-3-8B-INSTRUCT	4	2	2
OPENBIO-LLM-8B	4	2	2
LLAMA-3-8B	4	2	2
BIO-MISTRAL-7B	32	2	2
MISTRAL-7B-INSTRUCT-v0.1	32	2	2
BIO-MEDGPT-LM-7B	32	2	2
LLAMA-2-7B-CHAT	32	2	2

Table E10: i2b2 (CAD) SFT configs.

Model	$B$	# GPUs	ZeRO
MED42-v2-70B	2	8	3
OPENBIO-LLM-70B	2	8	3
LLAMA-3-70B-INSTRUCT	2	8	3
MEDI-TRON-70B	2	8	3
CLINICAL-CAMEL-70B	2	8	3
MED42-v1-70B	2	8	3
LLAMA-2-70B	2	8	3
MED42-v2-8B	2	2	2
LLAMA-3-8B-INSTRUCT	2	2	2
OPENBIO-LLM-8B	2	2	2
LLAMA-3-8B	2	2	2
BIO-MISTRAL-7B	4	2	2
MISTRAL-7B-INSTRUCT-v0.1	4	2	2
BIO-MEDGPT-LM-7B	4	2	2
LLAMA-2-7B-CHAT	4	2	2

Table E12: i2b2 (Obesity) SFT configs.

Model	$B$	# GPUs	ZeRO
MED42-v2-70B	1	8	3
OPENBIO-LLM-70B	1	8	3
LLAMA-3-70B-INSTRUCT	1	8	3
MEDI-TRON-70B	1	8	3
CLINICAL-CAMEL-70B	1	8	3
MED42-v1-70B	1	8	3
LLAMA-2-70B	1	8	3
MED42-v2-8B	2	2	2
LLAMA-3-8B-INSTRUCT	2	2	2
OPENBIO-LLM-8B	2	2	2
LLAMA-3-8B	2	2	2
BIO-MISTRAL-7B	4	2	2
MISTRAL-7B-INSTRUCT-v0.1	4	2	2
BIO-MEDGPT-LM-7B	4	2	2
LLAMA-2-7B-CHAT	4	2	2

## References

Griffin Adams, Mert Ketenci, Shreyas Bhave, Adler Perotte, and Noémie Elhadad. Zero-Shot Clinical Acronym Expansion via Latent Meaning Cells. In *Machine Learning for Health NeurIPS Workshop*, 2020.

Monica Agrawal, Stefan Hegselmann, Hunter Lang, Yoon Kim, and David Sontag. Large Language Models are Few-Shot Clinical Information Extractors. *Conference on Empirical Methods in Natural Language Processing (EMNLP)*, 2022.

Emily Alsentzer, John Murphy, William Boag, Wei-Hung Weng, Di Jindi, Tristan Naumann, and Matthew McDermott. Publicly Available Clinical BERT Embeddings. In *NAACL Clinical Natural Language Processing (ClinicalNLP) Workshop*, 2019.

Mohammed Altaf. Medical Instruction 120k, 2023. URL <https://huggingface.co/datasets/Mohammed-Altaf/medical-instruction-120k>.

Anas Awadalla, Irena Gao, Joshua Gardner, Jack Hessel, Yusuf Hanafy, Wanrong Zhu, Kalyani Marathe, Yonatan Bitton, Samir Gadre, Jenia Jitsev, Simon Kornblith, Pang Wei Koh, Gabriel Ilharco, Mitchell Wortsman, and Ludwig Schmidt. OpenFlamingo: An Open-Source Framework for Training Large Autoregressive Vision-Language Models. *arXiv:2308.01390*, 2023.

Dan Biderman, Jacob Portes, Jose Javier Gonzalez Ortiz, Mansheej Paul, Philip Greengard, Connor Jennings, Daniel King, Sam Havens, Vitaliy Chiley, Jonathan Frankle, Cody Blakeney, and John Patrick Cunningham. LoRA Learns Less and Forgets Less. *Transactions on Machine Learning Research (TMLR)*, 2024.

Elliot Bolton, Abhinav Venigalla, Michihiro Yasunaga, David Hall, Betty Xiong, Tony Lee, Roxana Daneshjou, Jonathan Frankle, Percy Liang, Michael Carbin, and Christopher D. Manning. BioMedLM: A 2.7B Parameter Language Model Trained On Biomedical Text. *arXiv:2403.18421*, 2024.

À Bravo, J Piñero, N Queralt-Rosinach, M Rautschka, and LI Furlong. Extraction of Relations Between Genes and Diseases from Text and Large-scale Data Analysis: Implications for Translational Research. *BMC Bioinformatics*, 16(55), 01 2015.

Tom Brown, Benjamin Mann, Nick Ryder, Melanie Subbiah, Jared D Kaplan, Prafulla Dhariwal, Arvind Neelakantan, Pranav Shyam, Girish Sastry, Amanda Askell, Sandhini Agarwal, Ariel Herbert-Voss, Gretchen Krueger, Tom Henighan, Rewon Child, Aditya Ramesh, Daniel Ziegler, Jeffrey Wu, Clemens Winter, Chris Hesse, Mark Chen, Eric Sigler, Mateusz Litwin, Scott Gray, Benjamin Chess, Jack Clark, Christopher Berner, Sam McCandlish, Alec Radford, Ilya Sutskever, and Dario Amodei. Language Models are Few-Shot Learners. In *Advances in Neural Information Processing Systems (NeurIPS)*, 2020.

Alberto Mario Ceballos-Arroyo, Monica Munnangi, Jiuding Sun, Karen Zhang, Jared McInerney, Byron C. Wallace, and Silvio Amir. Open (Clinical) LLMs are Sensitive to Instruction Phrasings. In *ACL Workshop on Biomedical Natural Language Processing (BioNLP)*, 2024.

Tuhin Chakrabarty, Christopher Hidey, and Kathy McKeown. IMHO Fine-Tuning Improves Claim Detection. In *Proceedings of the 2019 Conference of the North American Chapter of the Association for Computational Linguistics: Human Language Technologies, Volume 1 (Long and Short Papers)*, 2019.

Zeming Chen, Alejandro Hernández-Cano, Angelika Romanou, Antoine Bonnet, Kyle Mataba, Francesco Salvi, Matteo Pagliardini, Simin Fan, Andreas Köpf, Amirkeivan Mohtashami, Alexandre Sallinen, Alireza Sakhaeirad, Vinitra Swamy, Igor Krawczuk, Deniz Bayazit, Axel Marmet, Syrielle Montariol, Mary-Anne Hartley, Martin Jaggi, and Antoine Bosselut. MediTron-70B: Scaling Medical Pretraining for Large Language Models. *arXiv:2311.16079*, 2023.

Wei-Lin Chiang, Zhuohan Li, Zi Lin, Ying Sheng, Zhanghao Wu, Hao Zhang, Lianmin Zheng, Siyuan Zhuang, Yonghao Zhuang, Joseph E. Gonzalez, Ion Stoica, and Eric P. Xing. Vicuna: An Open-Source Chatbot Impressing GPT-4 with 90%\* ChatGPT Quality, March 2023. URL <https://lmsys.org/blog/2023-03-30-vicuna/>.

Clément Christophe, Praveen K Kanithi, Prateek Munjal, Tathagata Raha, Nasir Hayat, Ronnie Rajan, Ahmed Al-Mahrooqi, Avani Gupta, Muhammad Umar Salman, Gurpreet Gosal, Bhargav Kanakiya, Charles Chen, Natalia Vassilieva, Boulbaba Ben Amor, Marco AF Pimentel, and Shadab Khan. Med42 – Evaluating Fine-Tuning Strategies for Medical LLMs: Full-Parameter vs. Parameter-Efficient Approaches. *arXiv:2404.14779*, 2024a.

Clément Christophe, Praveen K Kanithi, Tathagata Raha, Shadab Khan, and Marco AF Pimentel. Med42-V2: A Suite of Clinical LLMs. *arXiv:2408.06142*, 2024b.

Tim Dettmers, Artidoro Pagnoni, Ari Holtzman, and Luke Zettlemoyer. QLoRA: Efficient Finetuning of Quantized LLMs. In *Advances in Neural Information Processing Systems (NeurIPS)*, 2023.

Jacob Devlin, Ming-Wei Chang, Kenton Lee, and Kristina Toutanova. BERT: Pre-training of Deep Bidirectional Transformers for Language Understanding. In *Proceedings of the 2019 Conference of the North American Chapter of the Association for Computational Linguistics: Human Language Technologies, Volume 1 (Long and Short Papers)*, 2019.

Rezarta Islamaj Doğan, Robert Leaman, and Zhiyong Lu. NCBI Disease Corpus: A Resource for Disease Name Recognition and Concept Normalization. *Journal of Biomedical Informatics*, 47:1–10, 2014.

Jason Fries, Ethan Steinberg, Scott Fleming, Michael Wornow, Yizhe Xu, Keith Morse, Dev Dash, and Nigam Shah. How Foundation Models Can Advance AI in Healthcare, December 2022a. URL <https://hai.stanford.edu/news/how-foundation-models-can-advance-ai-healthcare>.

Jason Fries, Leon Weber, Natasha Seelam, Gabriel Altay, Debajyoti Datta, Samuele Garda, Sunny Kang, Rosaline Su, Wojciech Kusa, Samuel Cahyawijaya, Fabio Barth, Simon Ott, Matthias Samwald, Stephen Bach, Stella Biderman, Mario Sänger, Bo Wang, Alison Callahan, Daniel León Periñán, Théo Gigant, Patrick Haller, Jenny Chim, Jose Posada, John

Giorgi, Karthik Rangasai Sivaraman, Marc Pàmies, Marianna Nezhurina, Robert Martin, Michael Cullan, Moritz Freidank, Nathan Dahlberg, Shubhanshu Mishra, Shamik Bose, Nicholas Broad, Yanis Labrak, Shlok Deshmukh, Sid Kiblawi, Ayush Singh, Minh Chien Vu, Trishala Neeraj, Jonas Golde, Albert Villanova del Moral, and Benjamin Beilharz. BigBio: A Framework for Data-Centric Biomedical Natural Language Processing. In *Advances in Neural Information Processing Systems (NeurIPS)*, 2022b.

Leo Gao, Stella Biderman, Sid Black, Laurence Golding, Travis Hoppe, Charles Foster, Jason Phang, Horace He, Anish Thite, Noa Nabeshima, Shawn Presser, and Connor Leahy. The Pile: An 800GB Dataset of Diverse Text for Language Modeling. *arXiv:2101.00027*, 2020.

Ary L. Goldberger, Luis A. N. Amaral, Leon Glass, Jeffrey M. Hausdorff, Plamen Ch. Ivanov, Roger G. Mark, Joseph E. Mietus, George B. Moody, Chung-Kang Peng, and H. Eugene Stanley. PhysioBank, PhysioToolkit, and PhysioNet: Components of a New Research Resource for Complex Physiologic Signals. *Circulation*, 101(23):e215–e220, June 2000.

Yu Gu, Robert Tinn, Hao Cheng, Michael Lucas, Naoto Usuyama, Xiaodong Liu, Tristan Naumann, Jianfeng Gao, and Hoifung Poon. Domain-Specific Language Model Pretraining for Biomedical Natural Language Processing. *Association for Computing Machinery (ACM) Transactions on Computing for Healthcare*, 3(1), Oct. 2021.

Suchin Gururangan, Ana Marasović, Swabha Swamydipta, Kyle Lo, Iz Beltagy, Doug Downey, and Noah A. Smith. Don’t Stop Pretraining: Adapt Language Models to Domains and Tasks. In Dan Jurafsky, Joyce Chai, Natalie Schluter, and Joel Tetreault, editors, *Annual Meeting of the Association for Computational Linguistics (ACL)*, 2020.

Tianyu Han, Lisa C Adams, Jens-Michalis Papaioannou, Paul Grundmann, Tom Oberhauser, Alexander Löser, Daniel Truhn, and Keno K Bressem. MedAlpaca—An Open-Source Collection of Medical Conversational AI Models and Training Data. *arXiv:2304.08247*, 2023.

Xuehai He, Yichen Zhang, Luntian Mou, Eric Xing, and Pengtao Xie. PathVQA: 30000+ Questions for Medical Visual Question Answering. *arXiv preprint arXiv:2003.10286*, 2020.

Dan Hendrycks, Collin Burns, Steven Basart, Andy Zou, Mantas Mazeika, Dawn Song, and Jacob Steinhardt. Measuring Massive Multitask Language Understanding. In *International Conference on Learning Representations (ICLR)*, 2021.

Evan Hernandez, Diwakar Mahajan, Jonas Wulff, Micah J Smith, Zachary Ziegler, Daniel Nadler, Peter Szolovits, Alistair Johnson, and Emily Alsentzer. Do We Still Need Clinical Language Models? In *Conference on Health, Inference, and Learning (CHIL)*, 2023.

Edward J Hu, Yelong Shen, Phillip Wallis, Zeyuan Allen-Zhu, Yuanzhi Li, Shean Wang, Lu Wang, and Weizhu Chen. LoRA: Low-Rank Adaptation of Large Language Models. In *International Conference on Learning Representations (ICLR)*, 2022.

Andrew Jaegle, Felix Gimeno, Andy Brock, Oriol Vinyals, Andrew Zisserman, and Joao Carreira. Perceiver: General Perception with Iterative Attention. In *International Conference on Machine Learning (ICML)*, 2021.

Daniel P. Jeong, Saurabh Garg, Zachary C. Lipton, and Michael Oberst. Medical Adaptation of Large Language and Vision-Language Models: Are We Making Progress? In *Conference on Empirical Methods in Natural Language Processing (EMNLP)*, 2024.

Albert Q. Jiang, Alexandre Sablayrolles, Arthur Mensch, Chris Bamford, Devendra Singh Chaplot, Diego de las Casas, Florian Bressand, Gianna Lengyel, Guillaume Lample, Lucile Saulnier, Lélio Renard Lavaud, Marie-Anne Lachaux, Pierre Stock, Teven Le Scao, Thibaut Lavril, Thomas Wang, Timothée Lacroix, and William El Sayed. Mistral 7B. *arXiv:2310.06825*, 2023.

Zhengbao Jiang, Frank F. Xu, Jun Araki, and Graham Neubig. How Can We Know What Language Models Know? *Transactions of the Association for Computational Linguistics*, 8:423–438, 2020.

Di Jin, Eileen Pan, Nassim Oufattolle, Wei-Hung Weng, Hanyi Fang, and Peter Szolovits. What Disease Does This Patient Have? A Large-scale Open Domain Question Answering Dataset from Medical Exams. *arXiv:2009.13081*, 2020.

Qiao Jin, Bhuwan Dhingra, Zhengping Liu, William Cohen, and Xinghua Lu. PubMedQA: A Dataset for Biomedical Research Question Answering. In Kentaro Inui, Jing Jiang, Vincent Ng, and Xiaojun Wan, editors, *Conference on Empirical Methods in Natural Language Processing and the International Joint Conference on Natural Language Processing (EMNLP-IJCNLP)*, 2019.

Alistair E.W. Johnson, Tom J. Pollard, Lu Shen, Li wei H. Lehman, Mengling Feng, Mohammad Ghassemi, Benjamin Moody, Peter Szolovits, Leo Anthony Celi, and Roger G. Mark. MIMIC-III, a Freely Accessible Critical Care Database. *Scientific Data*, 3(160035), 2016.

Diederik P. Kingma and Jimmy Ba. Adam: A Method for Stochastic Optimization. In *International Conference on Learning Representations (ICLR)*, 2015.

Leonard Konle and Fotis Jannidis. Domain and Task Adaptive Pretraining for Language Models. In *Workshop on Computational Humanities Research (CHR)*, 2020.

Martin Krallinger, Obdulia Rabal, Saber Ahmad Akhondi, Martín Pérez Pérez, Jesus Santamaría, Gael Pérez Rodríguez, Georgios Tsatsaronis, Ander Intxaurrendo, José Antonio Baso López, Umesh K. Nandal, Erin M. van Buel, Ambika Chandrasekhar, Marleen Rodenburg, Astrid Lægreid, Marius A. Doornenbal, Julen Oyarzábal, Anália Lourenço, and Alfonso Valencia. Overview of the BioCreative VI chemical-protein interaction Track. In *Proceedings of the BioCreative VI Workshop*, 2017.

Sunjun Kweon, Jiyoung Kim, Heeyoung Kwak, Dongchul Cha, Hangyul Yoon, Kwanghyun Kim, Jeewon Yang, Seunghyun Won, and Edward Choi. EHRNoteQA: An LLM Benchmark for Real-World Clinical Practice Using Discharge Summaries. *arXiv:2402.16040*, 2024.

Woosuk Kwon, Zhuohan Li, Siyuan Zhuang, Ying Sheng, Lianmin Zheng, Cody Hao Yu, Joseph E. Gonzalez, Hao Zhang, and Ion Stoica. Efficient Memory Management for Large

Language Model Serving with PagedAttention. In *ACM Symposium on Operating Systems Principles*, 2023.

Yanis Labrak, Adrien Bazoge, Emmanuel Morin, Pierre-Antoine Gourraud, Mickael Rouvier, and Richard Dufour. BioMistral: A Collection of Open-Source Pretrained Large Language Models for Medical Domains. *arXiv:2402.10373*, 2024.

Nathan Lambert, Lewis Tunstall, Nazneen Rajani, and Tristan Thrush. HuggingFace H4 Stack Exchange Preference Dataset, 2023. URL <https://huggingface.co/datasets/HuggingFaceH4/stack-exchange-preferences>.

Jason J. Lau, Soumya Gayen, Asma Ben Abacha, and Dina Demner-Fushman. A Dataset of Clinically Generated Visual Questions and Answers about Radiology Images. *Nature Scientific Data*, 5(180251), 2018.

Jinhyuk Lee, Wonjin Yoon, Sungdong Kim, Donghyeon Kim, Sunkyu Kim, Chan Ho So, and Jaewoo Kang. BioBERT: A Pre-trained Biomedical Language Representation Model for Biomedical Text Mining. *Bioinformatics*, 36(4):1234–1240, 2019.

Chunyuan Li, Cliff Wong, Sheng Zhang, Naoto Usuyama, Haotian Liu, Jianwei Yang, Tristan Naumann, Hoifung Poon, and Jianfeng Gao. LLaVA-Med: Training a Large Language-and-Vision Assistant for Biomedicine in One Day. In *Advances in Neural Information Processing Systems (NeurIPS) Datasets and Benchmarks Track*, 2023a.

Yunxiang Li, Zihan Li, Kai Zhang, Ruilong Dan, Steve Jiang, and You Zhang. ChatDoctor: A Medical Chat Model Fine-Tuned on a Large Language Model Meta-AI (LLaMA) Using Medical Domain Knowledge. *Cureus*, 15(6), 2023b.

Percy Liang, Rishi Bommasani, Tony Lee, Dimitris Tsipras, Dilara Soylu, Michihiro Yasunaga, Yian Zhang, Deepak Narayanan, Yuhuai Wu, Ananya Kumar, Benjamin Newman, Binhang Yuan, Bobby Yan, Ce Zhang, Christian Cosgrove, Christopher D. Manning, Christopher Ré, Diana Acosta-Navas, Drew A. Hudson, Eric Zelikman, Esin Durmus, Faisal Ladhak, Frieda Rong, Hongyu Ren, Huaxiu Yao, Jue Wang, Keshav Santhanam, Laurel Orr, Lucia Zheng, Mert Yuksekgonul, Mirac Suzgun, Nathan Kim, Neel Guha, Niladri Chatterji, Omar Khattab, Peter Henderson, Qian Huang, Ryan Chi, Sang Michael Xie, Shibani Santurkar, Surya Ganguli, Tatsunori Hashimoto, Thomas Icard, Tianyi Zhang, Vishrav Chaudhary, William Wang, Xuechen Li, Yifan Mai, Yuhui Zhang, and Yuta Koreeda. Holistic Evaluation of Language Models. *arXiv:2211.09110*, 2023.

Weixiong Lin, Ziheng Zhao, Xiaoman Zhang, Chaoyi Wu, Ya Zhang, Yanfeng Wang, and Weidi Xie. PMC-CLIP: Contrastive Language-Image Pre-training using Biomedical Documents. In *Medical Image Computing and Computer Assisted Intervention (MICCAI)*, 2023.

Bo Liu, Li-Ming Zhan, Li Xu, Lin Ma, Yan Yang, and Xiao-Ming Wu. SLAKE: A Semantically-Labeled Knowledge-Enhanced Dataset for Medical Visual Question Answering. *arXiv:2102.09542*, 2021.

Fenglin Liu, Bang Yang, Chenyu You, Xian Wu, Shen Ge, Zhangdaihong Liu, Xu Sun, Yang Yang, and David A. Clifton. Retrieve, Reason, and Refine: Generating Accurate and Faithful Patient Instructions. In *Advances in Neural Information Processing Systems (NeurIPS)*, 2022.

Haotian Liu, Chunyuan Li, Qingyang Wu, and Yong Jae Lee. Visual Instruction Tuning. In *Advances in Neural Information Processing Systems (NeurIPS)*, 2023.

Kyle Lo, Lucy Lu Wang, Mark Neumann, Rodney Kinney, and Daniel Weld. S2ORC: The semantic scholar open research corpus. In *Association for Computational Linguistics*, 2020.

Ilya Loshchilov and Frank Hutter. Decoupled Weight Decay Regularization. In *International Conference on Learning Representations (ICLR)*, 2019.

Renqian Luo, Lai Sun, Yingce Xia, Tao Qin, Sheng Zhang, Hoifung Poon, and Tie-Yan Liu. BioGPT: Generative Pre-trained Transformer for Biomedical Text Generation and Mining. In *Briefings in Bioinformatics*, 2022.

Yizhen Luo, Jiahuan Zhang, Siqi Fan, Kai Yang, Yushuai Wu, Mu Qiao, and Zaiqing Nie. BioMedGPT: Open Multimodal Generative Pre-trained Transformer for Biomedicine. *arXiv:2308.09442*, 2023.

Mason Marks and Claudia E. Haupt. AI Chatbots, Health Privacy, and Challenges to HIPAA Compliance. *Journal of American Medical Association (JAMA)*, 330(4):309–310, 07 2023.

Meta. Introducing Meta Llama 3: The Most Capable Openly Available LLM to Date, April 2024. URL <https://ai.meta.com/blog/meta-llama-3/>.

Sungrim Moon, Serguei Pakhomov, Nathan Liu, James O. Ryan, and Genevieve B. Melton. A Sense Inventory for Clinical Abbreviations and Acronyms Created Using Clinical Notes and Medical Dictionary Resources. *Journal of the American Medical Informatics Association*, 21(2):299–307, 03 2014.

Michael Moor, Oishi Banerjee, Zahra Shakeri, Harlan Krumholz, Jure Leskovec, Eric Topol, and Pranav Rajpurkar. Foundation Models for Generalist Medical Artificial Intelligence. *Nature*, 616:259–265, 2023a.

Michael Moor, Qian Huang, Shirley Wu, Michihiro Yasunaga, Cyril Zakka, Yash Dalmia, Eduardo Pontes Reis, Pranav Rajpurkar, and Jure Leskovec. Med-Flamingo: A Multi-modal Medical Few-shot Learner. *arXiv:2307.15189*, 2023b.

OpenAI. GPT-4 Technical Report. *arXiv:2303.08774*, 2023a.

OpenAI. GPT-4V(ision) System Card, September 2023b. URL <https://openai.com/contributions/gpt-4v/>.

Ankit Pal and Malaikannan Sankarasubbu. OpenBioLLMs: Advancing Open-Source Large Language Models for Healthcare and Life Sciences, 2024. URL <https://huggingface.co/aaditya/OpenBioLLM-Llama3-70B>.

Ankit Pal, Logesh Kumar Umapathi, and Malaikannan Sankarasubbu. MedMCQA: A Large-scale Multi-Subject Multi-Choice Dataset for Medical domain Question Answering. In *Conference on Health, Inference, and Learning (CHIL)*, 2022.

Ankit Pal, Pasquale Minervini, Andreas Geert Motzfeldt, Aryo Pradipta Gema, and Beatrice Alex. Open Medical LLM Leaderboard, 2024. URL [https://huggingface.co/spaces/openlifescienceai/open\\_medical\\_llm\\_leaderboard](https://huggingface.co/spaces/openlifescienceai/open_medical_llm_leaderboard).

Alec Radford, Jeff Wu, Rewon Child, David Luan, Dario Amodei, and Ilya Sutskever. Language Models are Unsupervised Multitask Learners. In *OpenAI Blog*, 2019.

Samyam Rajbhandari, Jeff Rasley, Olatunji Ruwase, and Yuxiong He. ZeRO: Memory Optimizations Toward Training Trillion Parameter Models. In *Proceedings of the International Conference for High Performance Computing, Networking, Storage and Analysis*, 2020.

Alexey Romanov and Chaitanya Shivade. Lessons from Natural Language Inference in the Clinical Domain. In *Conference on Empirical Methods in Natural Language Processing (EMNLP)*, 2018.

Khaled Saab, Tao Tu, Wei-Hung Weng, Ryutaro Tanno, David Stutz, Ellery Wulczyn, Fan Zhang, Tim Strother, Chunjong Park, Elahe Vedadi, Juanma Zambrano Chaves, Szu-Yeu Hu, Mike Schaeckermann, Aishwarya Kamath, Yong Cheng, David G. T. Barrett, Cathy Cheung, Basil Mustafa, Anil Palepu, Daniel McDuff, Le Hou, Tomer Golany, Luyang Liu, Jean baptiste Alayrac, Neil Houlsby, Nenad Tomasev, Jan Freyberg, Charles Lau, Jonas Kemp, Jeremy Lai, Shekoofeh Azizi, Kimberly Kanada, SiWai Man, Kavita Kulkarni, Ruoxi Sun, Siamak Shakeri, Luheng He, Ben Caine, Albert Webson, Natasha Latysheva, Melvin Johnson, Philip Mansfield, Jian Lu, Ehud Rivlin, Jesper Anderson, Bradley Green, Renee Wong, Jonathan Krause, Jonathon Shlens, Ewa Dominowska, S. M. Ali Esfandiari, Katherine Chou, Claire Cui, Oriol Vinyals, Koray Kavukcuoglu, James Manyika, Jeff Dean, Demis Hassabis, Yossi Matias, Dale Webster, Joelle Barral, Greg Corrado, Christopher Semturs, S. Sara Mahdavi, Juraj Gottweis, Alan Karthikesalingam, and Vivek Natarajan. Capabilities of Gemini Models in Medicine. *arXiv:2404.18416*, 2024.

Melanie Sclar, Yejin Choi, Yulia Tsvetkov, and Alane Suhr. Quantifying Language Models' Sensitivity to Spurious Features in Prompt Design or: How I Learned to Start Worrying About Prompt Formatting. In *International Conference on Learning Representations (ICLR)*, 2024.

Karan Singhal, Shekoofeh Azizi, Tao Tu, S. Mahdavi, Jason Wei, Hyung Chung, Nathan Scales, Ajay Tanwani, Heather Cole-Lewis, Stephen Pfohl, Perry Payne, Martin Seneviratne, Paul Gamble, Chris Kelly, Abubakr Babiker, Nathanael Schärli, Aakanksha Chowdhery, Philip Mansfield, Dina Demner-Fushman, and Vivek Natarajan. Large Language Models Encode Clinical Knowledge. *Nature*, 620:1–9, 2023a.

Karan Singhal, Tao Tu, Juraj Gottweis, Rory Sayres, Ellery Wulczyn, Le Hou, Kevin Clark, Stephen Pfohl, Heather Cole-Lewis, Darlene Neal, Mike Schaeckermann, Amy Wang, Mohamed Amin, Sami Lachgar, Philip Mansfield, Sushant Prakash, Bradley Green, Ewa Dominowska, Blaise Aguera y Arcas, Nenad Tomasev, Yun Liu, Renee Wong, Christopher

Semturs, S. Sara Mahdavi, Joelle Barral, Dale Webster, Greg S. Corrado, Yossi Matias, Shekoofeh Azizi, Alan Karthikesalingam, and Vivek Natarajan. Towards Expert-Level Medical Question Answering with Large Language Models. *arXiv:2305.09617*, 2023b.

Ross Taylor, Marcin Kardas, Guillem Cucurull, Thomas Scialom, Anthony Hartshorn, Elvis Saravia, Andrew Poulton, Viktor Kerkez, and Robert Stojnic. Galactica: A Large Language Model for Science. *arXiv:2211.09085*, 2022.

Augustin Toma, Patrick R. Lawler, Jimmy Ba, Rahul G. Krishnan, Barry B. Rubin, and Bo Wang. Clinical Camel: An Open Expert-Level Medical Language Model with Dialogue-Based Knowledge Encoding. *arXiv:2305.12031*, 2023.

Hugo Touvron, Thibaut Lavril, Gautier Izacard, Xavier Martinet, Marie-Anne Lachaux, Timothée Lacroix, Baptiste Rozière, Naman Goyal, Eric Hambro, Faisal Azhar, Aurelien Rodriguez, Armand Joulin, Edouard Grave, and Guillaume Lample. LLaMA: Open and Efficient Foundation Language Models. *arXiv:2302.13971*, 2023a.

Hugo Touvron, Louis Martin, Kevin Stone, Peter Albert, Amjad Almahairi, Yasmine Babaei, Nikolay Bashlykov, Soumya Batra, Prajjwal Bhargava, Shruti Bhosale, Dan Bikel, Lukas Blecher, Cristian Canton Ferrer, Moya Chen, Guillem Cucurull, David Esiobu, Jude Fernandes, Jeremy Fu, Wenyin Fu, Brian Fuller, Cynthia Gao, Vedanuj Goswami, Naman Goyal, Anthony Hartshorn, Saghar Hosseini, Rui Hou, Hakan Inan, Marcin Kardas, Viktor Kerkez, Madiam Khabsa, Isabel Kloumann, Artem Korenev, Punit Singh Koura, Marie-Anne Lachaux, Thibaut Lavril, Jenya Lee, Diana Liskovich, Yinghai Lu, Yuning Mao, Xavier Martinet, Todor Mihaylov, Pushkar Mishra, Igor Molybog, Yixin Nie, Andrew Poulton, Jeremy Reizenstein, Rashi Rungta, Kalyan Saladi, Alan Schelten, Ruan Silva, Eric Michael Smith, Ranjan Subramanian, Xiaoqing Ellen Tan, Binh Tang, Ross Taylor, Adina Williams, Jian Xiang Kuan, Puxin Xu, Zheng Yan, Iliyan Zarov, Yuchen Zhang, Angela Fan, Melanie Kambadur, Sharan Narang, Aurelien Rodriguez, Robert Stojnic, Sergey Edunov, and Thomas Scialom. Llama 2: Open Foundation and Fine-Tuned Chat Models. *arXiv:2307.09288*, 2023b.

Tao Tu, Shekoofeh Azizi, Danny Driess, Mike Schaeckermann, Mohamed Amin, Pi-Chuan Chang, Andrew Carroll, Charles Lau, Ryutaro Tanno, Ira Ktena, Anil Palepu, Basil Mustafa, Aakanksha Chowdhery, Yun Liu, Simon Kornblith, David Fleet, Philip Mansfield, Sushant Prakash, Renee Wong, Sunny Virmani, Christopher Semturs, S. Sara Mahdavi, Bradley Green, Ewa Dominowska, Blaise Aguera y Arcas, Joelle Barral, Dale Webster, Greg S. Corrado, Yossi Matias, Karan Singhal, Pete Florence, Alan Karthikesalingam, and Vivek Natarajan. Towards Generalist Biomedical AI. *New England Journal of Medicine (NEJM) AI*, 1(3), 2024.

Özlem Uzuner. Recognizing Obesity and Comorbidities in Sparse Data. *Journal of the American Medical Informatics Association (JAMIA)*, 16(4):561–570, 2009.

Özlem Uzuner, Brett R South, Shuying Shen, and Scott L DuVall. 2010 i2b2/VA Challenge on Concepts, Assertions, and Relations in Clinical Text. *Journal of American Medical Informatics Association (JAMIA)*, 18(5):552–556, 06 2011.

Guan Wang, Sijie Cheng, Xianyuan Zhan, Xiangang Li, Sen Song, and Yang Liu. OpenChat: Advancing Open-source Language Models with Mixed-Quality Data. *arXiv:2309.11235*, 2024.

Lucy Lu Wang, Kyle Lo, Yoganand Chandrasekhar, Russell Reas, Jiangjiang Yang, Doug Burdick, Darrin Eide, Kathryn Funk, Yannis Katsis, Rodney Michael Kinney, Yunyao Li, Ziyang Liu, William Merrill, Paul Mooney, Dewey A. Murdick, Devvret Rishi, Jerry Sheehan, Zhihong Shen, Brandon Stilson, Alex D. Wade, Kuansan Wang, Nancy Xin Ru Wang, Christopher Wilhelm, Boya Xie, Douglas M. Raymond, Daniel S. Weld, Oren Etzioni, and Sebastian Kohlmeier. CORD-19: The COVID-19 Open Research Dataset. In *Proceedings of the 1st Workshop on NLP for COVID-19 at ACL 2020*, 2020.

Michael Wornow, Yizhe Xu, Rahul Thapa, Birju Patel, Ethan Steinberg, Scott Fleming, Michael A. Pfeffer, Jason Fries, and Nigam H. Shah. The Shaky Foundations of Large Language Models and Foundation Models for Electronic Health Records. *npj Digital Medicine*, 6(135), 7 2023.

Chaoyi Wu, Weixiong Lin, Xiaoman Zhang, Ya Zhang, Weidi Xie, and Yanfeng Wang. PMC-LLAMA: Toward Building Open-Source Language Models for Medicine. *Journal of the American Medical Informatics Association (JAMIA)*, page ocae045, 04 2024.

Chaojun Xiao, Xueyu Hu, Zhiyuan Liu, Cunchao Tu, and Maosong Sun. Lawformer: A Pre-trained Language Model for Chinese Legal Long Documents. *AI Open*, 2:79–84, 2021.

Lin Yang, Shawn Xu, Andrew Sellergren, Timo Kohlberger, Yuchen Zhou, Ira Ktena, Atilla Kiraly, Faruk Ahmed, Farhad Hormozdiari, Tiam Jaroensri, Eric Wang, Ellery Wulczyn, Fayaz Jamil, Theo Guidroz, Chuck Lau, Siyuan Qiao, Yun Liu, Akshay Goel, Kendall Park, Arnav Agharwal, Nick George, Yang Wang, Ryutaro Tanno, David G. T. Barrett, Wei-Hung Weng, S. Sara Mahdavi, Khaled Saab, Tao Tu, Sreenivasa Raju Kalidindi, Mozziyar Etemadi, Jorge Cuadros, Gregory Sorensen, Yossi Matias, Katherine Chou, Greg Corrado, Joelle Barral, Shravya Shetty, David Fleet, S. M. Ali Eslami, Daniel Tse, Shruthi Prabhakara, Cory McLean, Dave Steiner, Rory Pilgrim, Christopher Kelly, Shekoofeh Azizi, and Daniel Golden. Advancing Multimodal Medical Capabilities of Gemini. *arXiv:2405.03162*, 2024.

Xi Yang, Aokun Chen, Nima PourNejatian, Hoo Chang Shin, Kaleb E Smith, Christopher Parisien, Colin Compas, Cheryl Martin, AB Costa, Mona G Flores, Ying Zhang, Tanja Magoc, Christopher A Harle, Gloria Lipori, Duane A Mitchell, William R Hogan, Elizabeth A Shenkman, Jiang Bian, and Yonghui Wu. A Large Language Model for Electronic Health Records. *npj Digital Medicine*, 5(194), 12 2022.

Xiang Yue, Yuansheng Ni, Kai Zhang, Tianyu Zheng, Ruqi Liu, Ge Zhang, Samuel Stevens, Dongfu Jiang, Weiming Ren, Yuxuan Sun, Cong Wei, Botao Yu, Ruibin Yuan, Renliang Sun, Ming Yin, Boyuan Zheng, Zhenzhu Yang, Yibo Liu, Wenhao Huang, Huan Sun, Yu Su, and Wenhui Chen. MMMU: A Massive Multi-discipline Multimodal Understanding and Reasoning Benchmark for Expert AGI. In *Conference on Computer Vision and Pattern Recognition (CVPR)*, 2024.

Sheng Zhang, Yanbo Xu, Naoto Usuyama, Hanwen Xu, Jaspreet Bagga, Robert Tinn, Sam Preston, Rajesh Rao, Mu Wei, Naveen Valluri, Cliff Wong, Andrea Tupini, Yu Wang, Matt Mazzola, Swadheen Shukla, Lars Liden, Jianfeng Gao, Matthew P. Lungren, Tristan Naumann, Sheng Wang, and Hoifung Poon. BiomedCLIP: A Multimodal Biomedical Foundation Model Pretrained from Fifteen Million Scientific Image-Text Pairs. *arXiv:2303.00915*, 2023.

Tony Z. Zhao, Eric Wallace, Shi Feng, Dan Klein, and Sameer Singh. Calibrate Before Use: Improving Few-Shot Performance of Language Models. In *International Conference on Machine Learning (ICML)*, 2021.

Yanli Zhao, Andrew Gu, Rohan Varma, Liang Luo, Chien-Chin Huang, Min Xu, Less Wright, Hamid Shojanazeri, Myle Ott, Sam Shleifer, Alban Desmaison, Can Balioglu, Pritam Damania, Bernard Nguyen, Geeta Chauhan, Yuchen Hao, Ajit Mathews, and Shen Li. PyTorch FSDP: Experiences on Scaling Fully Sharded Data Parallel. *Proceedings of the VLDB Endowment*, 16(12):3848–3860, August 2023.